A Study on the Application of the Acoustic Emission Method for Steel Bridges

by

Kazuo Endo, B.E.

Thesis

Presented to the Faculty of the Graduate School

of The University of Texas at Austin

in Partial Fulfillment

of the Requirements

for the Degree of

Master of Science in Engineering

The University of Texas at Austin

December 2000

A Study on the Application of the Acoustic Emission Method for Steel Bridges

APPROVED BY

SUPERVISING COMMITTEE:

Supervisors: _____

Karl H. Frank

_____

Timothy J. Fowler

Acknowledgements

I would like to express my appreciation to all of those people who assisted me in the completion of this thesis: Mark F. Carlos and Dan. E Johnson of the Physical Acoustic Cooperation for helpful advice and providing us with the most up to date instrumentation, Blake Stasney for helping me to follow the necessary procedure during my experiment in the laboratory, Adnan Wasim for his assistance in solving the computer problems, Taichiro Okazaki for proofreading, Nat Ativitavas, Piya Chotickai, Michael J. Hagenberger and Marcel Poser for their assistance in performing my experiment. I wish to thank the Texas Department of Transportation for making bridges available. I would also like to express my gratitude to the Honshu-Shikoku Bridge Authority and the Express Highway Research Foundation of Japan for the financial support for my study and for my living expenses. I am very grateful to Dr. Timothy J. Fowler for his expert advice, encouragement and patience. Finally, I extend special thanks to Dr. Karl H. Frank for his tremendous amount of useful suggestions and encouragement on this thesis as well as his advice during my semesters.

December 8, 2000

Abstract

A STUDY ON THE APPLICATION OF THE ACOUSTIC EMISSION METHOD FOR STEEL BRIDGES

Kazuo Endo, M. S. E.

The University of Texas at Austin, 2000

Supervisors: Karl H. Frank
Timothy J. Fowler

This research presents an experimental application of the acoustic emission (AE) method to in-service steel bridges. Continuous AE monitoring of steel plates with an intentional notch was performed both in the field and in the laboratory using the guard sensor technique and the location technique. Results of this research show that the AE method is able to clearly and reliably detect the large crack both in the field and in the laboratory. The guard sensor technique and the location technique worked well. A filter was developed to eliminate the noise in the bridge test. The results indicate that the AE method has the potential to be a good inspection tool for in-service steel bridges.

Table of Contents

Acknowledgements iii

Abstract iv

List of Tables viii

List of Figures ix

CHAPTER 1. INTRODUCTION AND OVERVIEW 1

1.1 Introduction 1

1.2 Research Objectives 2

1.3 Research Program Overview 3

CHAPTER 2. LITERATURE REVIEW 6

2.1 Overview of Acoustic Emission 6

2.2 Applications of Acoustic Emission for Bridge Testing 8

2.3 Noise Discrimination 9

2.3.1 Swansong Filter 9

2.3.2 Guard Sensor Technique 11

2.4 Source Location Technique 12

2.5 Techniques Used in This Study 14

CHAPTER 3. BACKGROUND NOISE MONITORING 15

3.1 Introduction 15

3.2 Experimental Program 17

3.2.1 Instrumentation 17

3.2.2 Test Program 17
3.3 Results at the I-35 Bridge over 4th street 18
3.4 Results at the Texas-71 Bridge over US-183 25
3.5 Noise Discrimination Procedure 32
CHAPTER 4. STRESS MEASURING 34
4.1 Introduction 34
4.2 Experimental Program 34
4.2.1 Instrumentation 34
4.2.2 Test Program 35
4.3 Test Results for the Stress Measuring 35
CHAPTER 5. LABORATORY TEST 38
5.1 Introduction 38
5.2 Experimental Program for AE Monitoring of Fatigue Crack Growth (1) 38
5.2.1 Instrumentation 38
5.2.2 Specimen Details 39
5.2.3 Test Program 40
5.3 Experimental Program for AE Monitoring of Fatigue Crack Growth (2) 42
5.3.1 Instrumentation 42
5.3.2 Specimen Details 43
5.3.3 Test Program 44
5.4 Test Results for Laboratory Test 48
5.4.1 AE Monitoring of Fatigue Crack Growth (1) 48

5.4.1 AE Monitoring of Fatigue Crack Growth (2) 54
CHAPTER 6. FIELD TEST 59
6.1 Introduction 59
6.2 Experimental Program 59
6.3 Test Results for the Field Test 61
CHAPTER 7. CONCLUSIONS AND RECOMMENDATIONS 74
7.1 Conclusions 74
7.2 Recommendations 75
References 77
Vita 79

List of Tables

Table 3.1: Geometry of Bridges 15

Table 3.2: Hardware Set Up 18

Table 4.1: Maximum and Minimum Stresses 36

Table 5.1: Test Conditions of the 2nd Laboratory Test 46

Table 5.2: Hardware Set Up 47

Table 6.1: Test Conditions of the Field Test 60

List of Figures

Figure 2.1: Schema of the AE Process 7

Figure 2.2: Swansong Filter 10

Figure 2.3: Guard Sensor Concept 11

Figure 2.4: Principle of Linear Location 13

Figure 3.1: I-35 Bridge over 4th street 16

Figure 3.2: Texas-71 Bridge over US-183 16

Figure 3.3: Instrumentation 17

Figure 3.4: Period 1 (I-35 Bridge over 4th street) 19

Figure 3.5: Period 2 (I-35 Bridge over 4th street) 20

Figure 3.6: Period 3 (I-35 Bridge over 4th street) 21

Figure 3.7: Period 4 (I-35 Bridge over 4th street) 22

Figure 3.8: Period 5 (I-35 Bridge over 4th street) 23

Figure 3.9: Duration-Amplitude (after applying Swansong II and III filter) .. 24

Figure 3.10: Period 1 (Texas-71 Bridge over US-183) 26

Figure 3.11: Period 2 (Texas-71 Bridge over US-183) 27

Figure 3.12: Period 3 (Texas-71 Bridge over US-183) 28

Figure 3.13: Period 4 (Texas-71 Bridge over US-183) 29

Figure 3.14: Period 5 (Texas-71 Bridge over US-183) 30

Figure 3.15: Period 6 (Texas-71 Bridge over US-183) 31

Figure 4.1: Instrumentation 35

Figure 4.2: Stresses of 10-minute Measuring (Period 2, 2nd girder) 36

Figure 4.3: Stress Variation During 10 Seconds (Period 2, 2nd girder)..... 37

Figure 5.1: Specimen Geometry and Sensor Location (1) 40

Figure 5.2: Overall View of AE Monitoring of Fatigue Crack Growth (1) 41

Figure 5.3: Instrumentation (LAM) 42

Figure 5.4: Specimen Geometry and Sensor Location (2) 43

Figure 5.5: Elevation of AE Monitoring of Fatigue Crack Growth (2) 45

Figure 5.6: Overall View of AE Monitoring of Fatigue Crack Growth (2) 48

Figure 5.7: AE from Growing Fatigue Crack (R15I)..... 49

Figure 5.8: AE from Growing Fatigue Crack (R30I)..... 50

Figure 5.9: Fatigue Crack..... 51

Figure 5.10: Cumulative Amplitude Distribution (R15I) 52

Figure 5.11: Correlation Between Crack Growth and AE (R15I) 53

Figure 5.12: Location Display (Case 1) 55

Figure 5.13: Location Display (Case 2) 55

Figure 5.14: Location Display (Case 3) 55

Figure 5.15: Duration-Amplitude (Case 1) 56

Figure 5.16: Duration-Amplitude (Case 2) 56

Figure 5.17: Duration-Amplitude (Case 3) 56

Figure 6.1: Overall View of Field Test 61

Figure 6.2: Location Display (Period 1, Cracked Plate) 62
Figure 6.3: Location Display (Period 1, Plane Plate)..... 62
Figure 6.4: Location Display (Period 2, Cracked Plate) 63
Figure 6.5: Location Display (Period 2, Plane Plate)..... 63
Figure 6.6: Location Display (Period 3, Cracked Plate) 64
Figure 6.7: Duration-Amplitude (Period 1, Cracked Plate) 64
Figure 6.8: Duration-Amplitude (Period 1, Plane Plate)..... 65
Figure 6.9: Duration-Amplitude (Period 2, Cracked Plate) 65
Figure 6.10: Duration-Amplitude (Period 2, Plane Plate)..... 66
Figure 6.11: Duration-Amplitude (Period 3, Cracked Plate) 66
Figure 6.12: Result of the Background Noise Monitoring..... 68
Figure 6.12: Location Display (Period 1, Cracked Plate, After Filtering)..... 70
Figure 6.13: Location Display (Period 1, Plane Plate, After Filtering) 70
Figure 6.14: Location Display (Period 2, Cracked Plate, After Filtering)..... 71
Figure 6.15: Location Display (Period 2, Plane Plate, After Filtering) 71
Figure 6.16: Location Display (Period 3, Cracked Plate, After Filtering)..... 72

CHAPTER 1. INTRODUCTION AND OVERVIEW

1.1 Introduction

Although the importance of bridge maintenance is widely recognized, bridge inspection technology has not progressed as rapidly as in other fields. A bridge collapse may cause a catastrophic result and huge loss of property. The representative accident so far is the Silver Bridge accident in 1967 at Point Pleasant, killed 47 people, and it is said that the cost of this disaster was 175 million dollars (Prine 1995). When tragic failures occur, the interest and concern reaches a temporary peak, but then subsides with time unfortunately. Reliable and integrated inspection technology for detecting localized deterioration, defects and damage in bridge members is needed to prevent such tragedy.

Currently, most highway bridge inspection is done using visual inspection. This method cannot help but rely heavily on subjective evaluations based on the experience and the skill of inspectors. Besides, this method may be expensive and time-consuming even if a single structure element is inspected because of access limitations to various parts of a bridge structure. Frank points out that we should develop nondestructive inspection techniques, which are automated and not subject to subjective inspector interpretation (Frank 1993). In recent years the acoustic emission (AE) method has been considered as one of the

useful inspection tools for in-service steel bridges, meeting the above demands (e.g., Chase 1995, Sison *et al.* 1996).

Although the AE method has existed for a long time, its use in bridge inspection has been limited as compared to other nondestructive testing methods. Each method has particular advantages and limitations that determine its appropriateness for a specific inspection application. It is said that the AE method is more advantageous than other methods for detecting crack growth, continuous monitoring and locating remote or hidden flaws (Lozev *et al*. 1997).

Since the 1970's, a variety of field and laboratory tests had been performed to confirm the feasibility and applicability of this method to steel bridge inspection. These studies showed that AE method could be used successfully to monitor fatigue cracks in in-service steel bridges and determine whether they are growing or not (Pollock 1995). However, Pollock also suggested that further data accumulation under variable conditions should be performed.

1.2 Research Objectives

The most serious obstacle to the successful and regular use of the AE method in steel bridge inspection is noise discrimination. Because we cannot easily stop the traffic just for inspection purposes, we are obliged to inspect the bridge in the presence of interfering background noise which is not related to

crack growth. Unwanted noise, which is associated bolt fretting and rubbing or traffic, must be distinguished systematically from sounds associated with crack initiation or growth.

The objective of this research is to study and characterize the AE associated with a fatigue crack both in a relatively quiet environment (laboratory) and in a typical bridge environment. This research seeks to establish the correlation between fatigue crack growth and AE parameters and locate the fatigue crack position by using AE activity both in an in-service bridge and in the laboratory. The results reported from this research will provide the technical basis of the effectiveness of AE method as an inspection tool of in-service steel bridges.

1.3 Research Program Overview

This research presents an experimental application of the AE method to in-service steel bridges. Continuous AE monitoring of steel plates with an intentional notch was performed both in the field and in the laboratory. In the field, the specimen was mounted on the lower flange at mid-span of the girder by clamps and AE from the crack was monitored continuously during normal traffic loading. At the same time, AE monitoring of a plane steel plate was done as well. In the laboratory, the same situation is reproduced: the same specimen was mounted on the bigger steel plate that simulates the flange of the bridge, and AE

was monitored continuously by the same instrument during cyclic loading generated by a fatigue machine. To eliminate interfering background noise from source other than the crack, and to locate the crack position, the guard sensor technique (described in 2.3.2) and the location technique (described in 2.3.3) were adopted.

Prior to these tests, background noise monitoring and stress measuring of in-service bridges, and AE monitoring of a laboratory fatigue test was conducted. Background noise monitoring is carried out at two sites to see the traffic or other source related noise as well as to determine the noise discrimination procedure. The service stress was measured in the bridge where the continuous AE monitoring was performed to determine the stress range for the laboratory test and to confirm that the crack length was long enough so that the crack could grow in the field test. AE monitoring of the fatigue test was performed to establish the correlation between fatigue crack growth and AE parameters in the laboratory.

The remainder of this thesis is organized into six chapters. Chapter 2 contains background information on the AE testing of steel bridges and a literature review of material relevant to this area of study. Chapters 3 and 4 describe the experimental program and test results on background monitoring and stress measuring under normal traffic condition of in-service bridges. Chapter 5 focuses on the experimental program and test results on two types of the fatigue

tests in the laboratory. Chapter 6 follows the same format and discusses the tests conducted on a field bridge. Finally, this thesis is concluded by Chapter 7 with a discussion of key findings from this study and suggestions for future research.

CHAPTER 2. LITERATURE REVIEW

In this chapter, principles of acoustic emission (AE) including noise discrimination and source location technique are briefly described. In addition, the history of the application of AE to steel bridges is introduced.

2.1 Overview of Acoustic Emission

AE is defined as a transient elastic wave generated within a material by means of the rapid release of energy from a localized source (ASTM 1999). When a material is subjected to a force, the resulting stress becomes the stimulus and produces local plastic deformation, and breakdown of the material at specific places. The material breakdown produces AE, which travels outward from the source, echoing through the body until it arrives at a sensor. The sensor translates the sound energy into an electrical signal, which is passed to electronic equipment for further processing. The AE process is schematized in Figure 2.1.

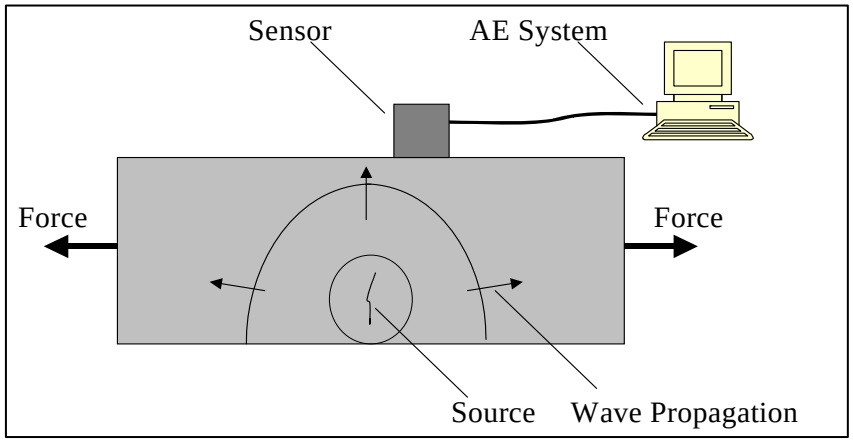

Source: PAC (2000)

Figure 2.1 Schema of the AE Process

During fatigue tests, AE is produced not only by the onset of yielding at the crack tip or crack extension, but also by the rubbing of fatigue crack surfaces due to closure (1973 Morton). Abrading surfaces emit frequent AE which have a slow rise time and a low amplitude. AE from crack closure can occur even during tension-tension cyclic loading (1972 Adams).

Since the AE method doesn't require energy input, other than the affected load, into the specimen to observe the response, it is classified as a passive nondestructive testing while other methods, such as radiography method or ultrasonic method, are classified as active methods (Bray and Stanley 1997). In other words, the AE method can be conducted under the influence of a typical loading environment.

2.2 Applications of Acoustic Emission for Bridge Testing

The first application of the AE method for testing bridges was done in 1971 by Pollock and Smith, while other nondestructive testing methods, such as ultrasonic method or dye penetrant method have been used for a longer time as standard inspection tools for steel bridges (Pollock and Smith 1972). They showed that signals measured in the field could be associated with test results in the laboratory. Following this test, several tests have been performed to characterize AE signals from flaws and various noises (Sison *et al.* 1996). A series of field tests was performed by the Virginia Department of Transportation and by the Federal Highway Administration (FHWA) (Lozev *et al.* 1997, Pollock 1995). In these studies, the characteristics of the AE method are summarized as follows:

(1) The AE method can detect actively growing flaws while other methods require periodic inspection to make sure whether a crack is active or not. Since repair of existing cracks can sometimes do more harm than good to a structure, it is necessary to determine whether a defect is benign or active before repairs are made.

(2) The AE method can locate remote or hidden flaws. This excludes the need for direct and close access to the locations of defects.

(3) The AE method is one of the few NDE (nondestructive examination) methods which are appropriate for long-term continuous monitoring of

flaws. The AE method is more sensitive than other NDE and can detect even incipient flaws. Other methods, which are highly dependent on defect size or surface opening, can reliably detect defects only after they have progressed beyond a certain size.

On the other hand, several problems are pointed out as follows:

(1) Unwanted noise due to traffic or other sources must be distinguished systematically from sounds associated with crack initiation or growth.

(2) The strategies that can accomplish cost-effective inspection are needed. From the cost-effectiveness point of view, it is unrealistic to apply the AE method to the whole structure. By focusing on defined critical areas, the advantages of the AE method are fully exploited.

(3) More field tests should be conducted to characterize AE in field bridges. Bridges are complex structures, with many structural boundaries, such as stiffeners, diaphragms, and so on. The way AE waves are transmitted and reflected in such details needs to be confirmed.

2.3 Noise Discrimination

2.3.1 Swansong Filter

The Association of American Railroads (AAR) developed a procedure for removing data which gives a false or nonrelevant indication, or extraneous noise (AAR 1999). The Swansong Filter utilize a technique which takes advantage of

specific characteristics of unwanted hits; hits arising from sliding or mechanical rubbing typically have long duration and low amplitude. Although these filters are used for tank cars, they may be applicable to bridges as well because the mechanism of noise occurrence is similar. The Swansong II and III Filters are defined as follows:

If (A_i-A_{th})<5 dB and D_i>2 ms
or (A_i-A_{th})<10 dB and D_i>3.5 ms } Criteria
or (A_i-A_{th})<15 dB and D_i>4.5 ms
eliminate all hits during the period (sec)
(T_i-T) to (T_i+T)
(Swansong II Filter: T=0.5 sec, Swansong III Filter: T=0.1 sec)

where:
A_i = Amplitude of Hits (dB)
A_{th} = Data Acquisition Threshold (dB)
D_i = Hit Duration (ms)
T_i = Arrival Time (sec)

The Swansong criteria listed above are shown schematically in Figure 2.2 for a threshold equal to 40 dB. Data above and to the left of the dashed line corresponds to the criteria.

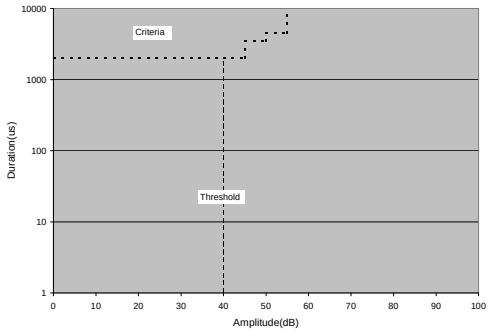

Figure 2.2 Swansong Filter

2.3.2 Guard Sensor Technique

The idea of the guard sensor technique was developed in the early 1960's (1995 Pollock). The concept of this technique is illustrated in Figure 2.3.

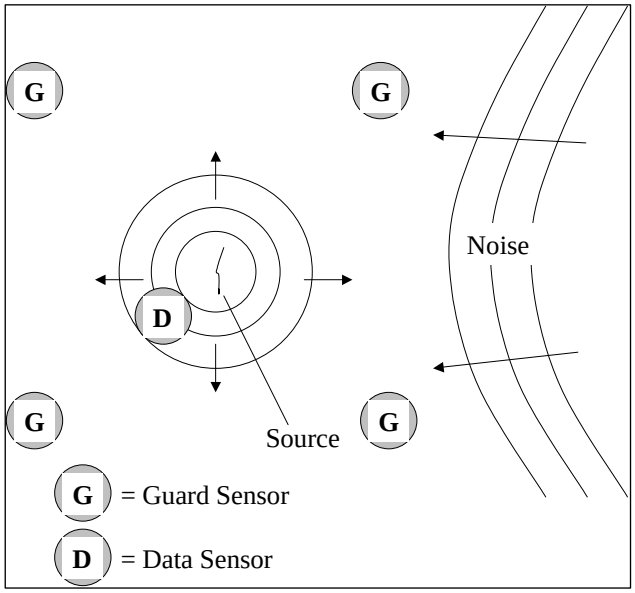

Source: PAC (2000)

Figure 2.3 Guard Sensor Concept

A data sensor is placed on the area of interest, surrounded by several guard sensors. AE waves from the area of interest will arrive at or hit the data sensor before hitting any of the guard sensors. Waves from outside the area of interest will hit at least one of the guard sensors before they hit the data sensor. By shutting down the data sensor for a certain period when the wave hits the guard sensor first, all hits on the data sensor which are coming from outside are not recorded.

The lockout time is defined as the minimum time before the software will resume processing of the data sensor. This should be equal to or exceed the time it takes an AE to travel the distance between the data sensor and the guard sensor. Generally it is calculated by following equation.

Lockout time (sec) = (D/V) x 1.2

Where
D = Distance between the Data Sensor and the Guard Sensor (in)
V = Velocity of Wave (in/sec) (=120,000 in/sec for steel)

Lozev (1997) and Pollock (1995) used the guard sensor technique in their bridge studies.

2.4 Source Location Technique

Source location capability is considered one of the advantages of AE for this application. A single event can be captured by several sensors as successive hits on those sensors. The difference of the arrival times tells us the location of the source. The principle of linear location is shown in Figure 2.4.

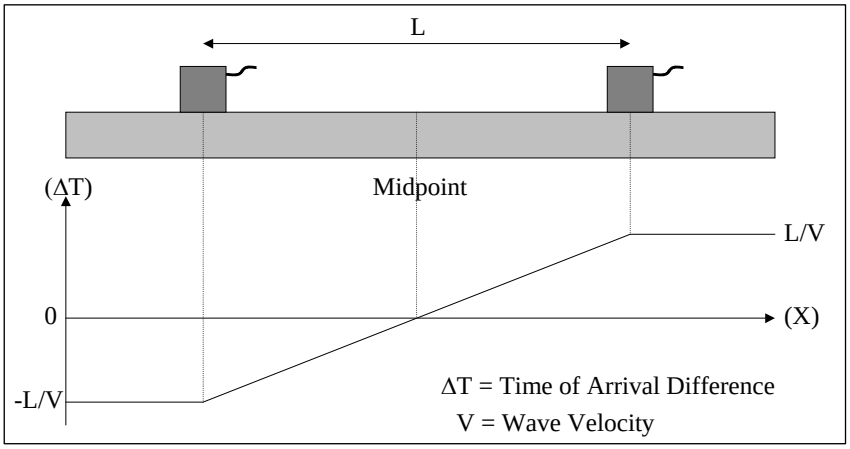

Source: PAC (2000)

Figure 2.4 Principle of Linear Location

If the source is at the midpoint, AE hits occur on both sensors simultaneously and ΔT is zero. As the source moves away from the midpoint, the ΔT varies in proportion to the distance moved. The relationship is linear:

$$X = \Delta T \times V/2$$

When the source is beyond one of the sensors, ΔT takes a constant value of $\pm L/V$. In other words, a source between the sensors can be located, but a source beyond the sensors is incorrectly calculated as being located at the first hit sensor.

There are two timing methods depending on the definition of the arrival time of hits. One is First Threshold Crossing Method (FTC), which measures the arrival time difference based on when the threshold is exceeded. The other is Peak Timing Method (PT), in which the arrival time is taken as the time of the

peak amplitude. Since peak time is independent of amplitude as opposed to FTC, PT might result in a more accurate location (PAC 2000).

Lozev (1997) and Pollock (1995) used the source location technique in their bridge studies.

2.5 Techniques Used in This Study

Techniques used in this research are as follows:

(1) Swansong Filter

(2) Guard Sensor Technique

(3) Source Location Technique

CHAPTER 3. BACKGROUND NOISE MONITORING

3.1 Introduction

As discussed earlier, noise discrimination is an indispensable issue for successful use of the AE method in steel bridges. In order to assess the traffic and other non-structured source related noise, 15-minute background noise monitoring was carried out at two sites: one was the I-35 Bridge over 4th street (see Figure 3.1), the other was the Texas-71 Bridge over US-183 (see Figure 3.2). Both of these bridges have heavy traffic. Based on these tests, a noise discrimination procedure was determined. The geometry of these bridges is summarized in Table 3.1. The descriptions of the rolled sections are approximate and done by matching the measurement to the specified dimensions.

Table 3.1 Geometry of Bridges

	I-35 Bridge	Texas-71 Bridge
Type	Non-composite 5 span continuous rolled girder bridge	Non-composite 5 span continuous rolled girder bridge
Approximate Spans (ft.)	45+60+60+60+45	35+50+35+50+35
# of girders	8	6
Approximate Girder spacing (ft.)	8	8
Approximate Rolled Section	W27 x 114	W27 x 129
Bearing	Steel rocker	Steel rocker

Figure 3.1 I-35 Bridge over 4th street

Figure 3.2 Texas-71 Bridge over US-183

3.2 Experimental Program

3.2.1 Instrumentation

Data were collected using a 4-channel Physical Acoustic Corporation LOCAN-320 acoustic emission instrument and 150 kHz resonant sensors (R15I) and 300 kHz resonant sensors (R30I) with integral preamplifier. The sensors were mounted on the beam using magnetic hold-downs. In order to accomplish good acoustic contact between the sensor face and the beam, vacuum grease was used.

Figure 3.3 Instrumentation

3.2.2 Test Program

15-minute monitoring was preformed using 2 channels under the normal bridge traffic. At the I-35 Bridge over 4th street, the noise at the end of the girder near the bearing was recorded, while the noise at middle of the girder was recorded at the Texas-71 Bridge over US-183. The type and the location of the

sensor of each period are tabulated in Section 3.3 and 3.4. The hardware set up is summarized in Table 3.2.

Table 3.2 Hardware Set Up

Quantity	Values
Peak Definition Time (PDT)	200 μs
Hit Definition Time (HDT)	400 μs
Hit Lockout Time (HLT)	200 μs
Threshold	40 dB
Gain	23 dB
Sensor Preamplifier Gain (R15I)	40 dB
Sensor Preamplifier Gain (R30I)	40 dB
Instrument Bandpass Filter	3 kHz-1000 kHz
Sensor Bandpass Filter (R15I)	100-300 kHz
Sensor Bandpass Filter (R30I)	215-490 kHz

3.3 Results at the I-35 Bridge over the 4th street

Time-amplitude, time-energy, duration-amplitude (all three plots are before applying the Swansong Filter (see Section 2.3.1)), duration-amplitude (after applying the Swansong II Filter) during each 15-minute monitoring period are plotted in Figure 3.4 through Figure 3.8. The average amount of heavy trucks during each period was 48. One of the duration-amplitude (after applying the Swansong III Filter) relationships is shown in the Figure 3.9.

Channel 1

Sensor	# of Hits	Max. of Amplitude	Max. of Energy
R15I	1323	84(dB)	4380

Channel 2

Sensor	# of Hits	Max. of Amplitude	Max. of Energy
R15I	3091	81(dB)	6945

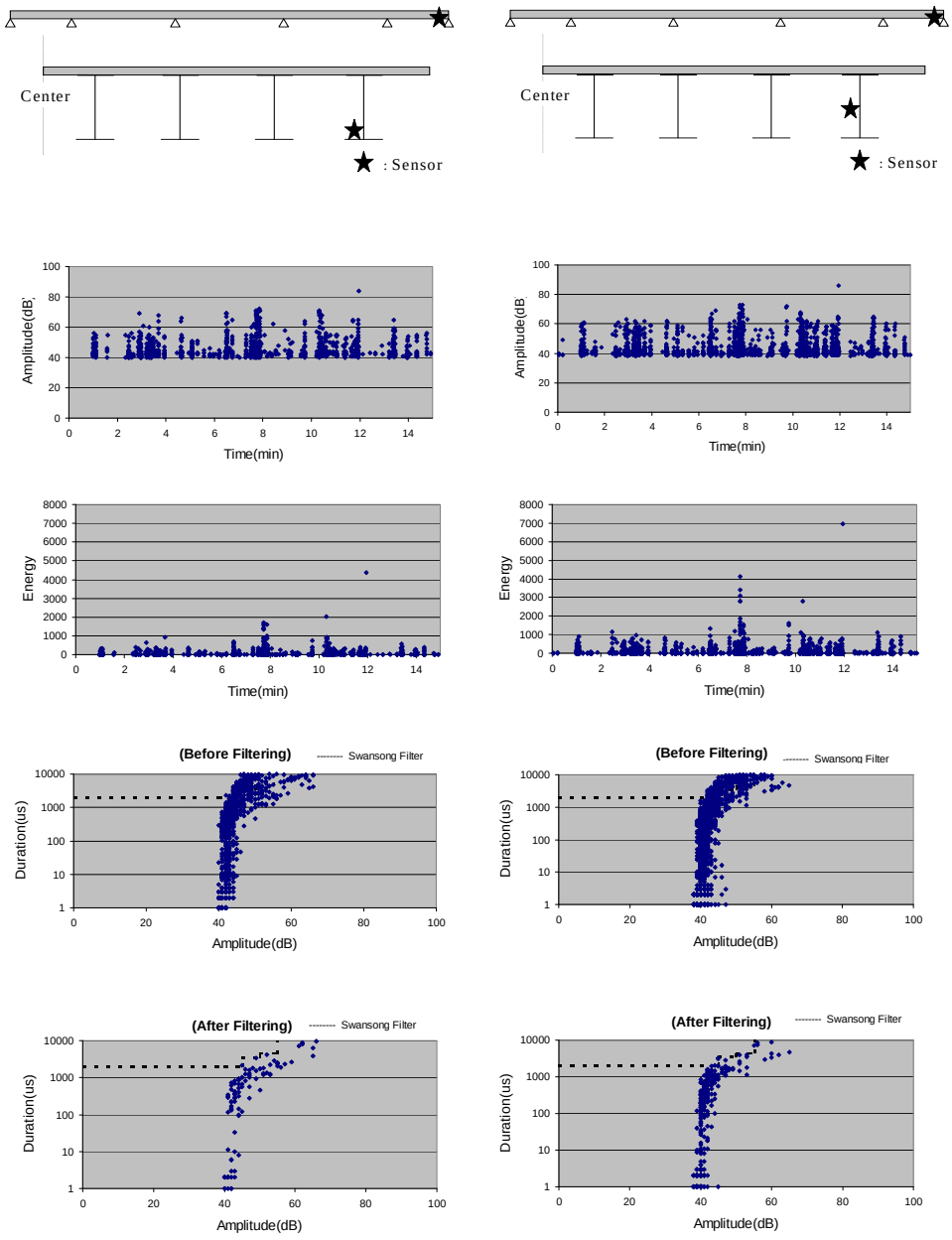

Figure 3.4 Period 1 (I-35 Bridge over 4th street)

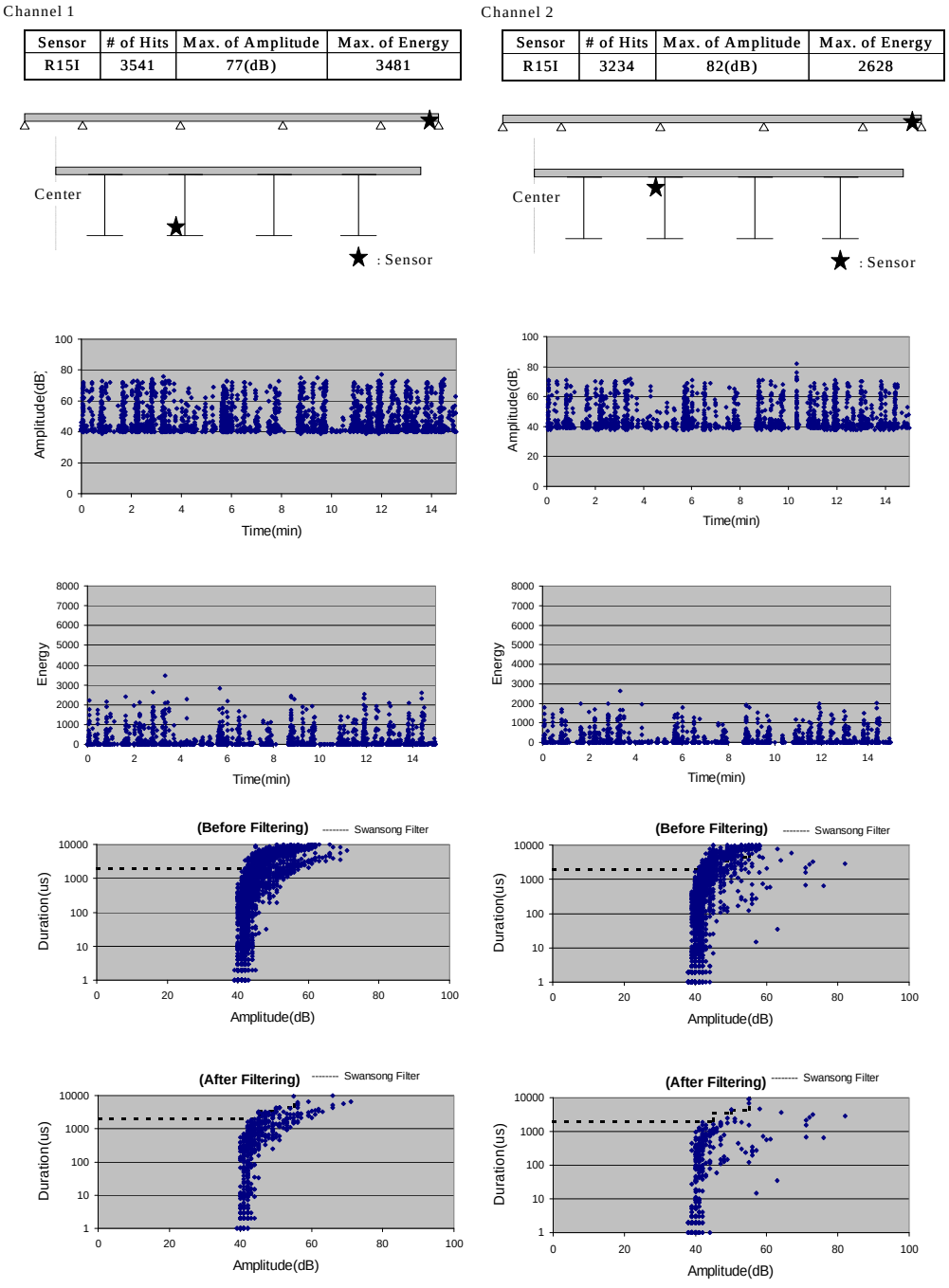

Figure 3.5 Period 2 (I-35 Bridge over 4th street)

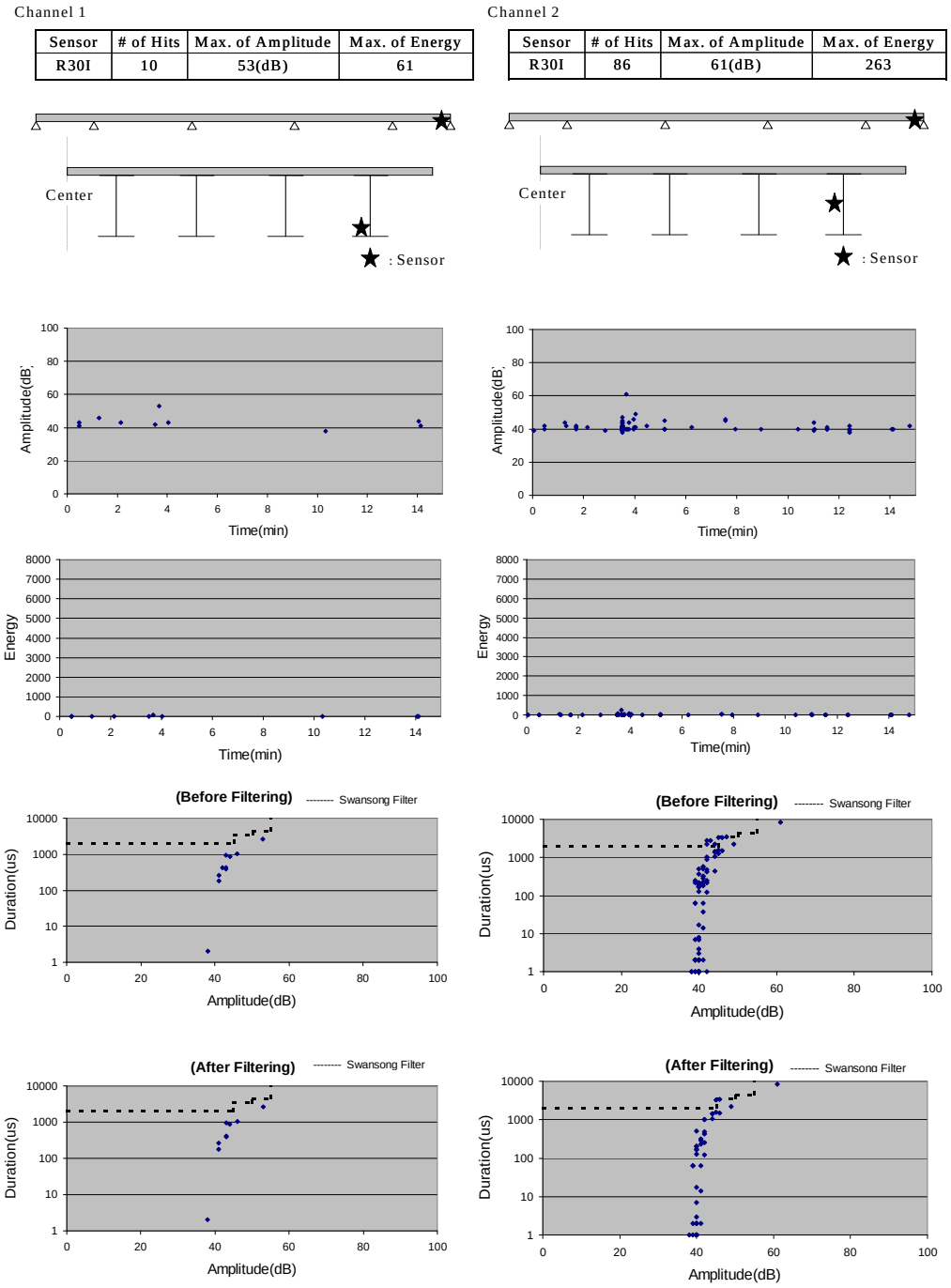

Figure 3.6 Period 3 (I-35 Bridge over 4th street)

Channel 1

Sensor	# of Hits	Max. of Amplitude	Max. of Energy
R30I	98	63(dB)	223

Channel 2

Sensor	# of Hits	Max. of Amplitude	Max. of Energy
R30I	766	71(dB)	904

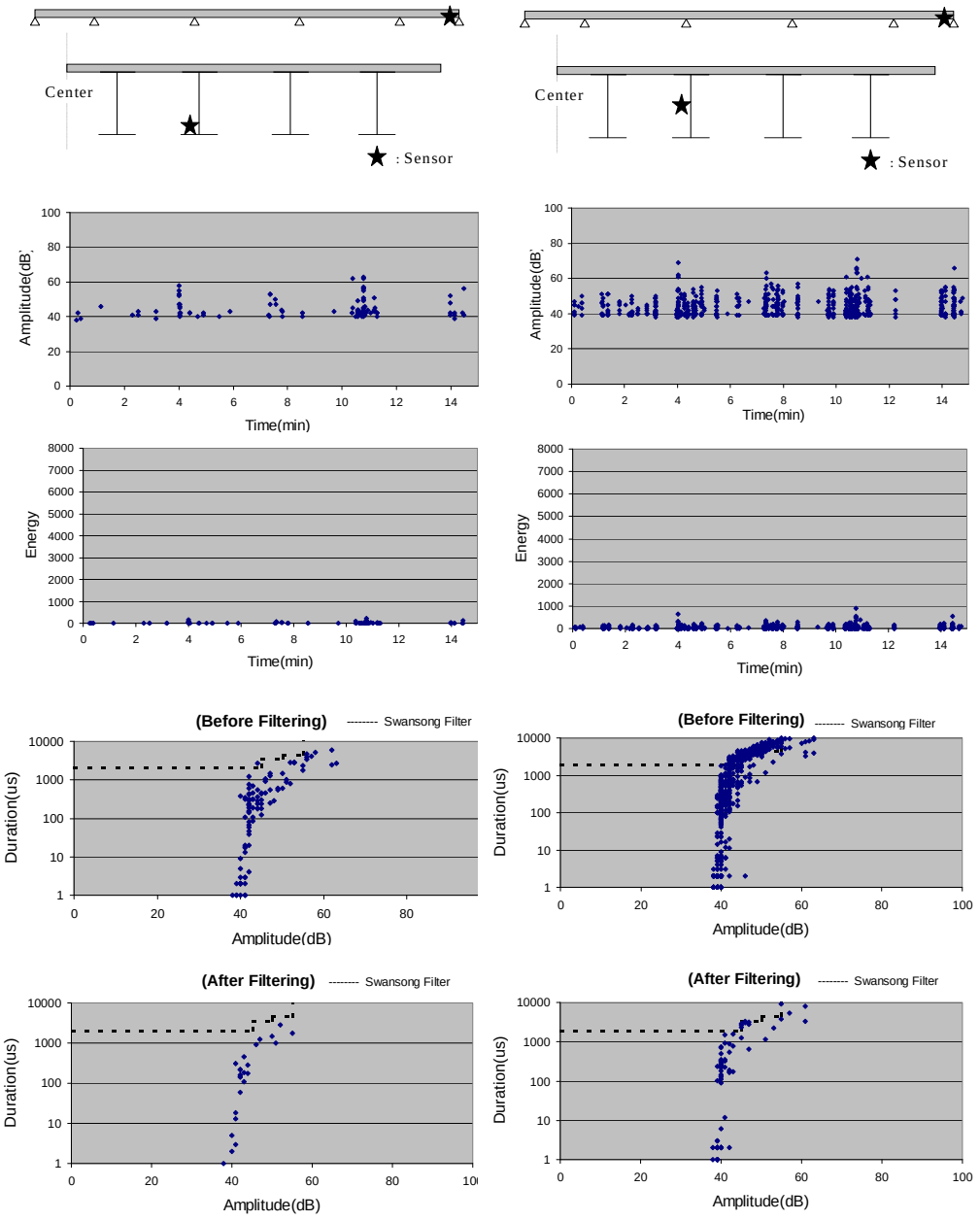

Figure 3.7 Period 4 (I-35 Bridge over 4th street)

Channel 1

Sensor	# of Hits	Max. of Amplitude	Max. of Energy
R30I	44	61(dB)	93

Channel 2

Sensor	# of Hits	Max. of Amplitude	Max. of Energy
R30I	228	59(dB)	182

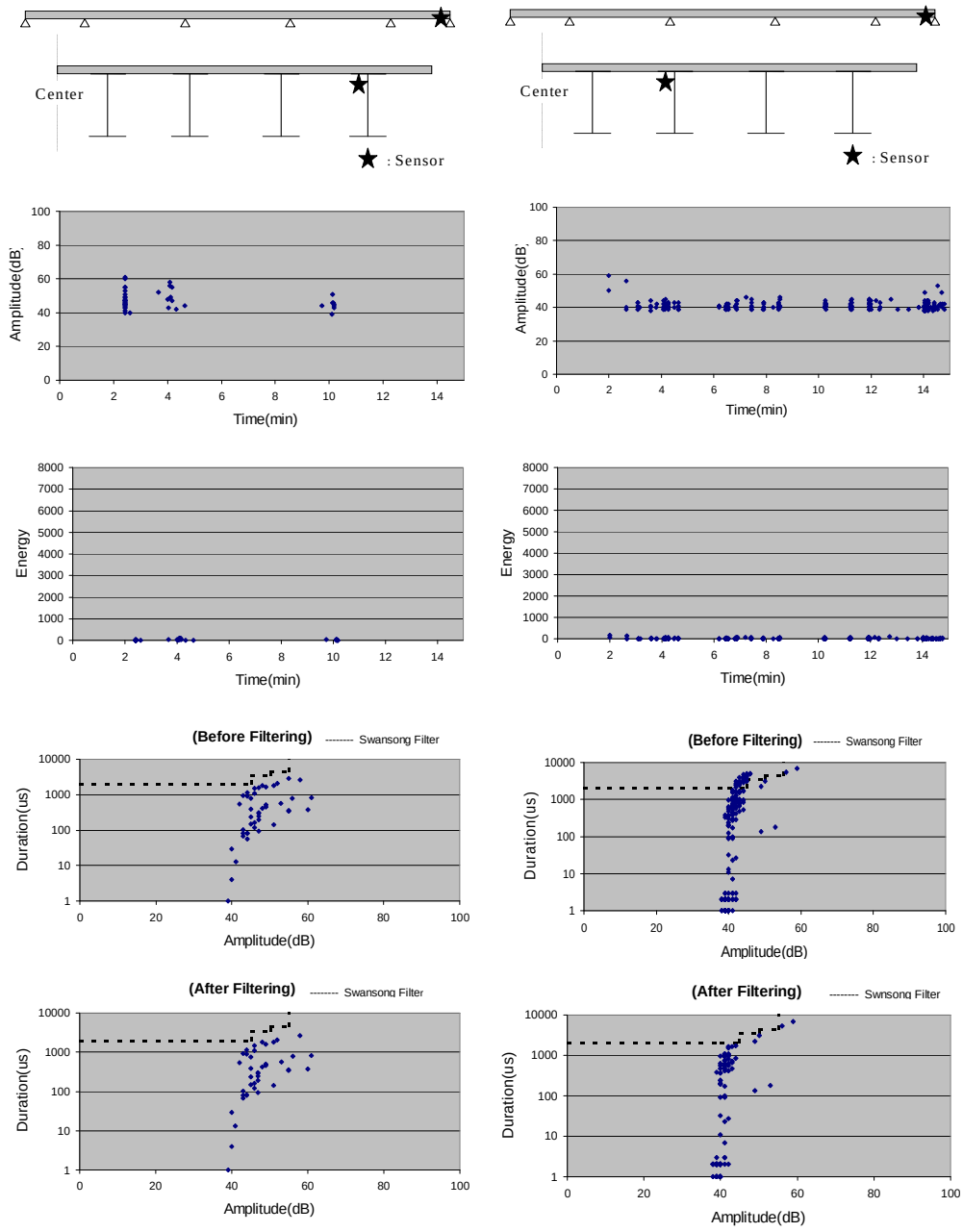

Figure 3.8 Period 5 (I-35 Bridge over 4th street)

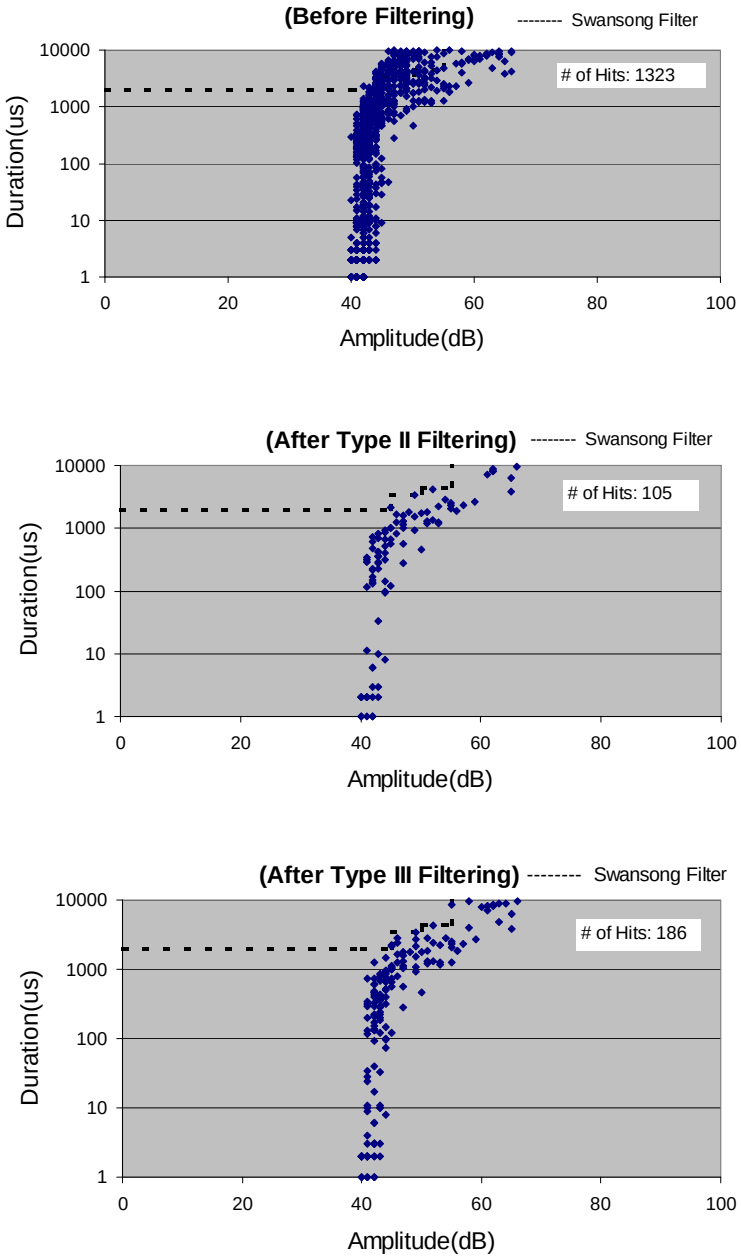

Figure 3.9 Duration-Amplitude (after applying Swansong II and III filter) [Period 1, Channel 1]

The R30I sensor, the higher frequency transducer, did not capture as much noise as the R15I sensor. This is caused by the fact that higher frequencies are attenuated more than lower frequencies. The maximum amplitude of the signal was about 60 dB for R30I, 80 dB for R15I. The minimum amplitude of the signal was 38 dB even though the threshold was 40dB. This is inherent in the older instruments, and has to do with the circuitry. The newer instruments have a software cut-off that eliminates anything below the threshold. Period 5 indicates that the 3rd girder from the outside was noisier than far outside girder. As Period 1, 3, 4 indicate, the web was noisier than the lower flange. Although the Swansong II and III Filter did reduce the noise data by 63% and 50% on average respectively, it could not eliminate the noise data completely. The remaining data seems to come mainly from the impact due to moving vehicles.

3.4 Results at the Texas-71 Bridge over US-183

Figure 3.10 through Figure 3.15 show the results at the Texas-71 Bridge in the same manner as at the I-35 Bridge. The average amount of heavy trucks during the 15-minute monitoring period was 38, which was less than at the I-35 Bridge.

Channel 1

Sensor	# of Hits	Max. of Amplitude	Max. of Energy
R30I	53	71(dB)	323

Channel 2

Sensor	# of Hits	Max. of Amplitude	Max. of Energy
R30I	105	83(dB)	7775

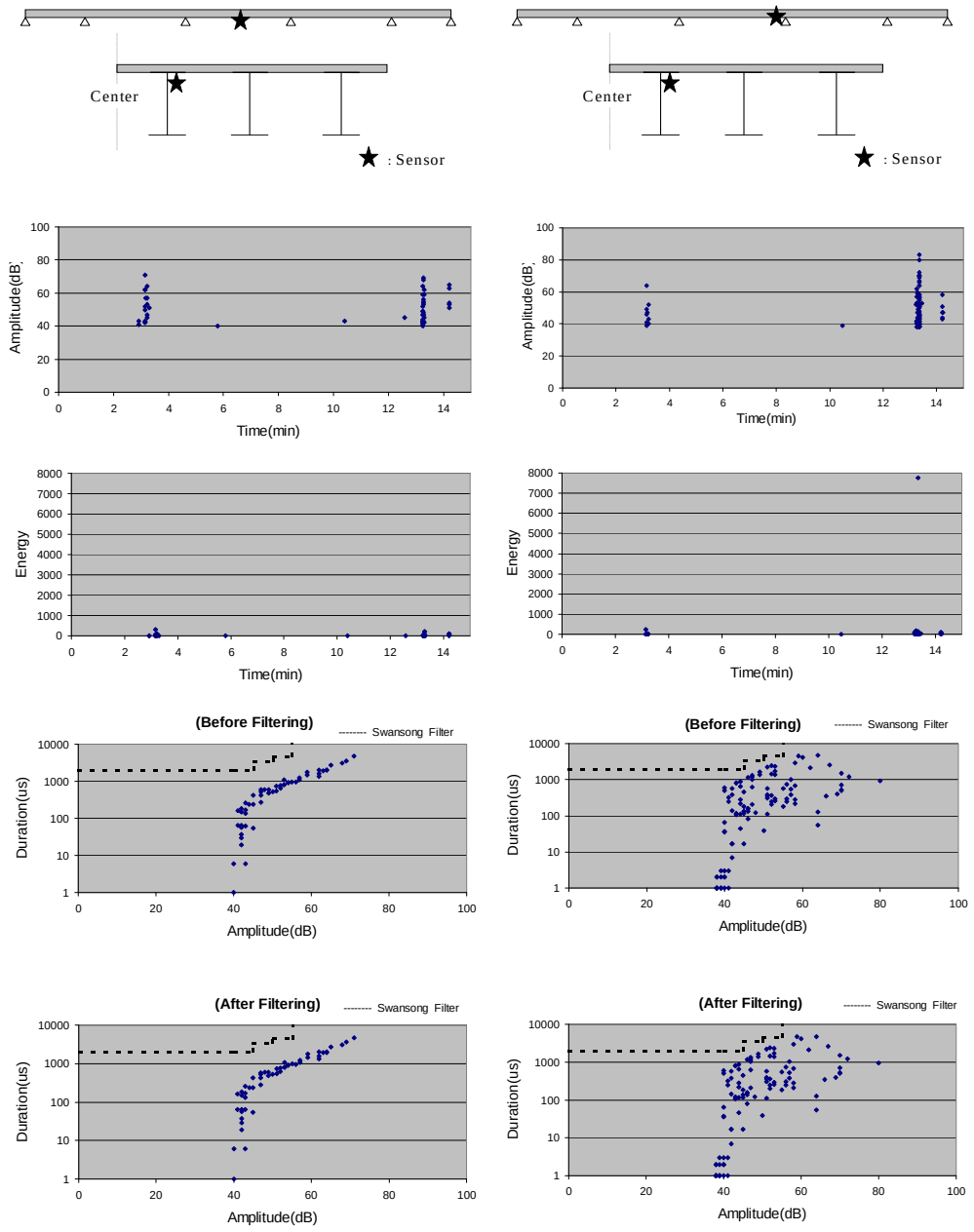

Figure 3.10 Period 1 (Texas-71 Bridge over US-183)

Channel 1

Sensor	# of Hits	Max. of Amplitude	Max. of Energy
R30I	45	60(dB)	150

Channel 2

Sensor	# of Hits	Max. of Amplitude	Max. of Energy
R30I	91	71(dB)	341

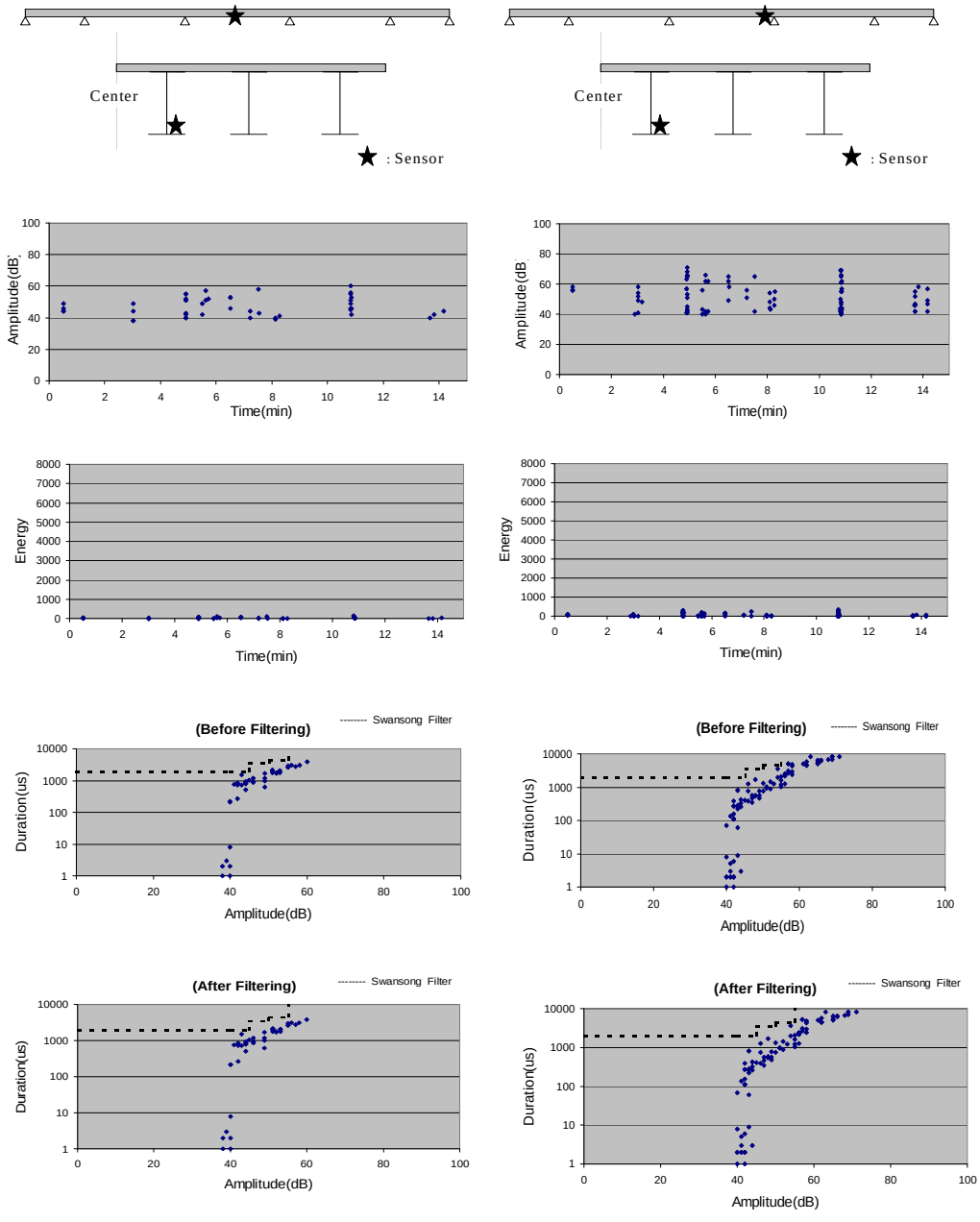

Figure 3.11 Period 2 (Texas-71 Bridge over US-183)

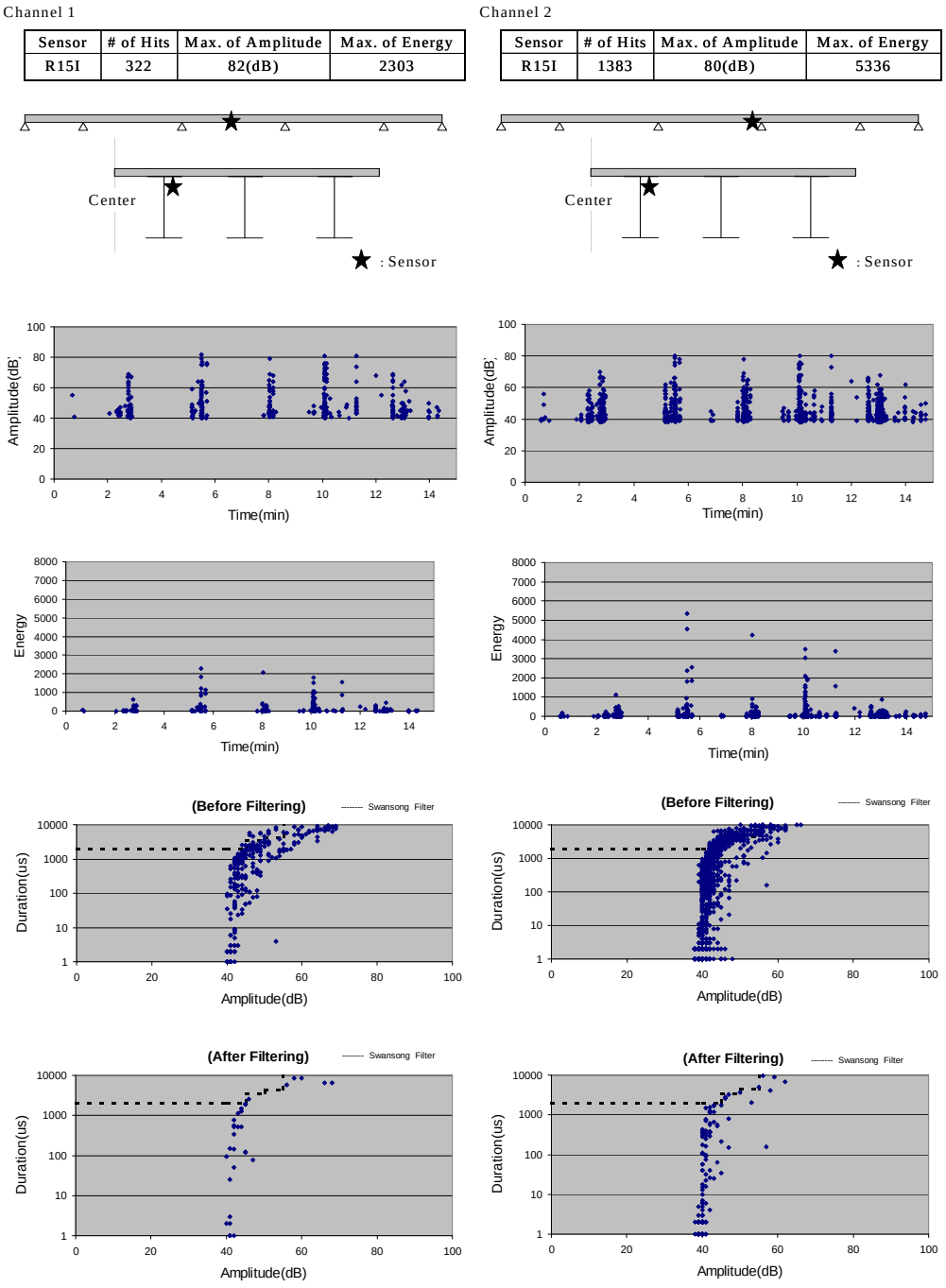

Figure 3.12 Period 3 (Texas-71 Bridge over US-183)

Channel 1

Sensor	# of Hits	Max. of Amplitude	Max. of Energy
R15I	812	90(dB)	5000

Channel 2

Sensor	# of Hits	Max. of Amplitude	Max. of Energy
R15I	3213	85(dB)	16643

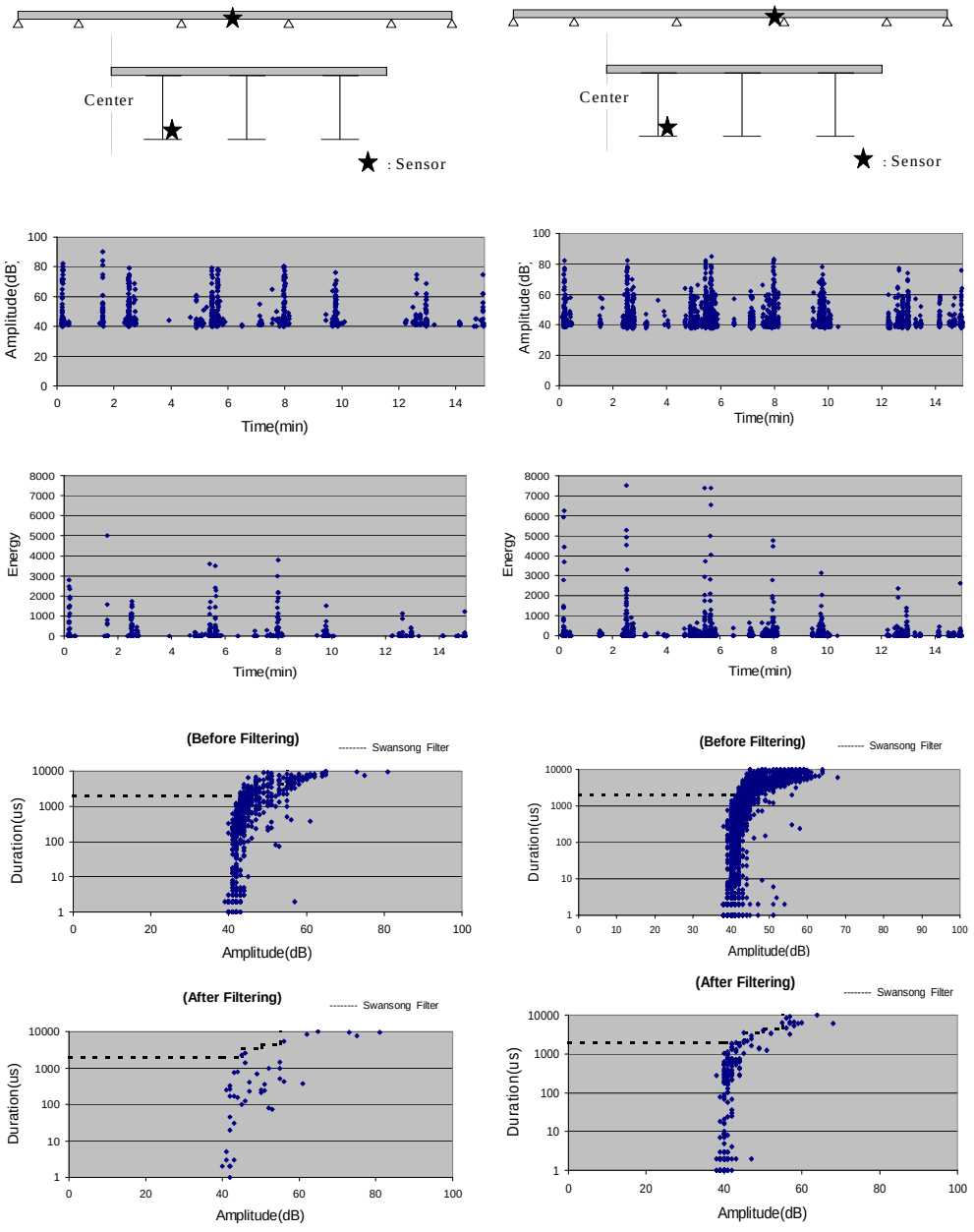

Figure 3.13 Period 4 (Texas-71 Bridge over US-183)

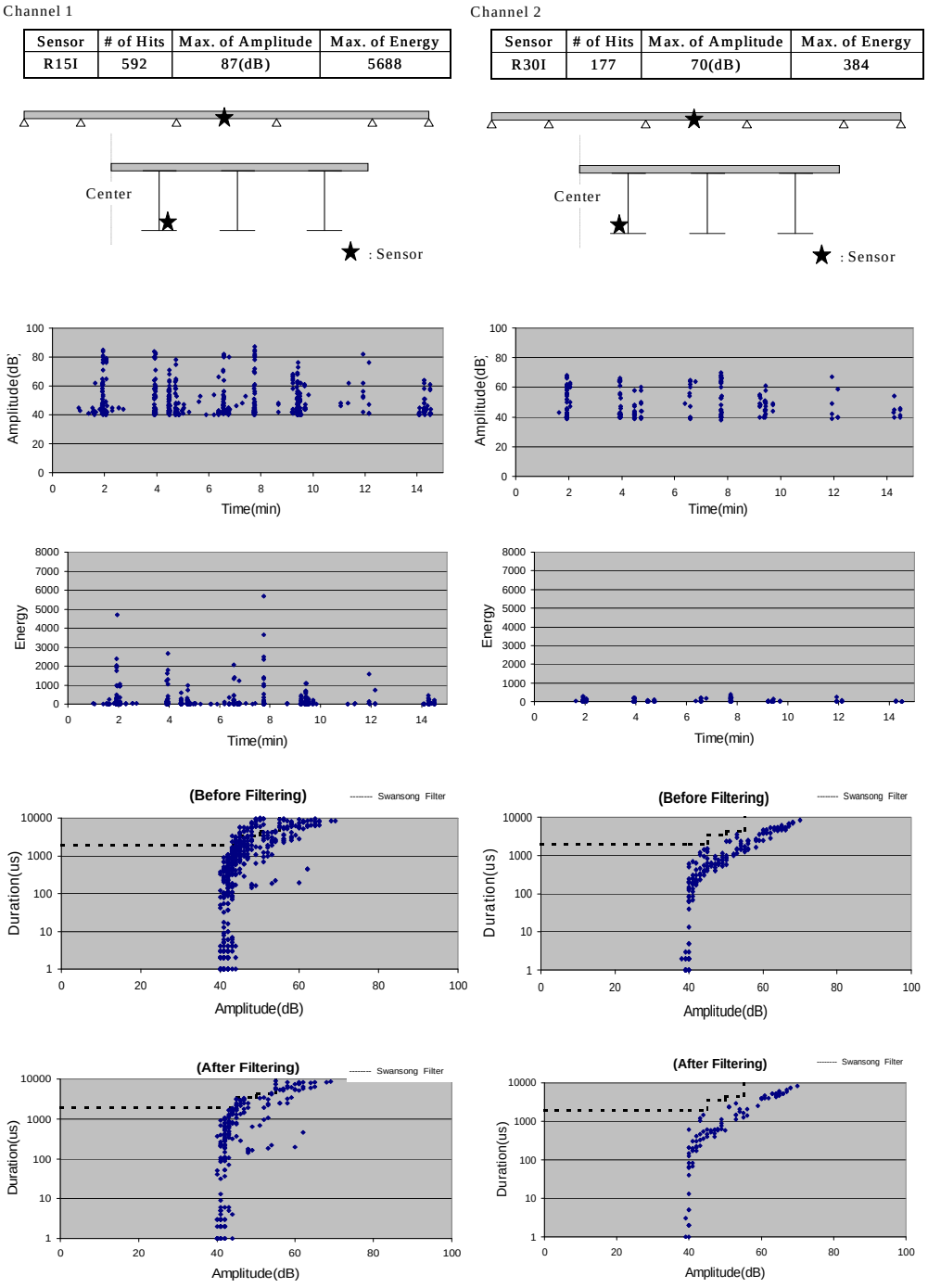

Figure 3.14 Period 5 (Texas-71 Bridge over US-183)

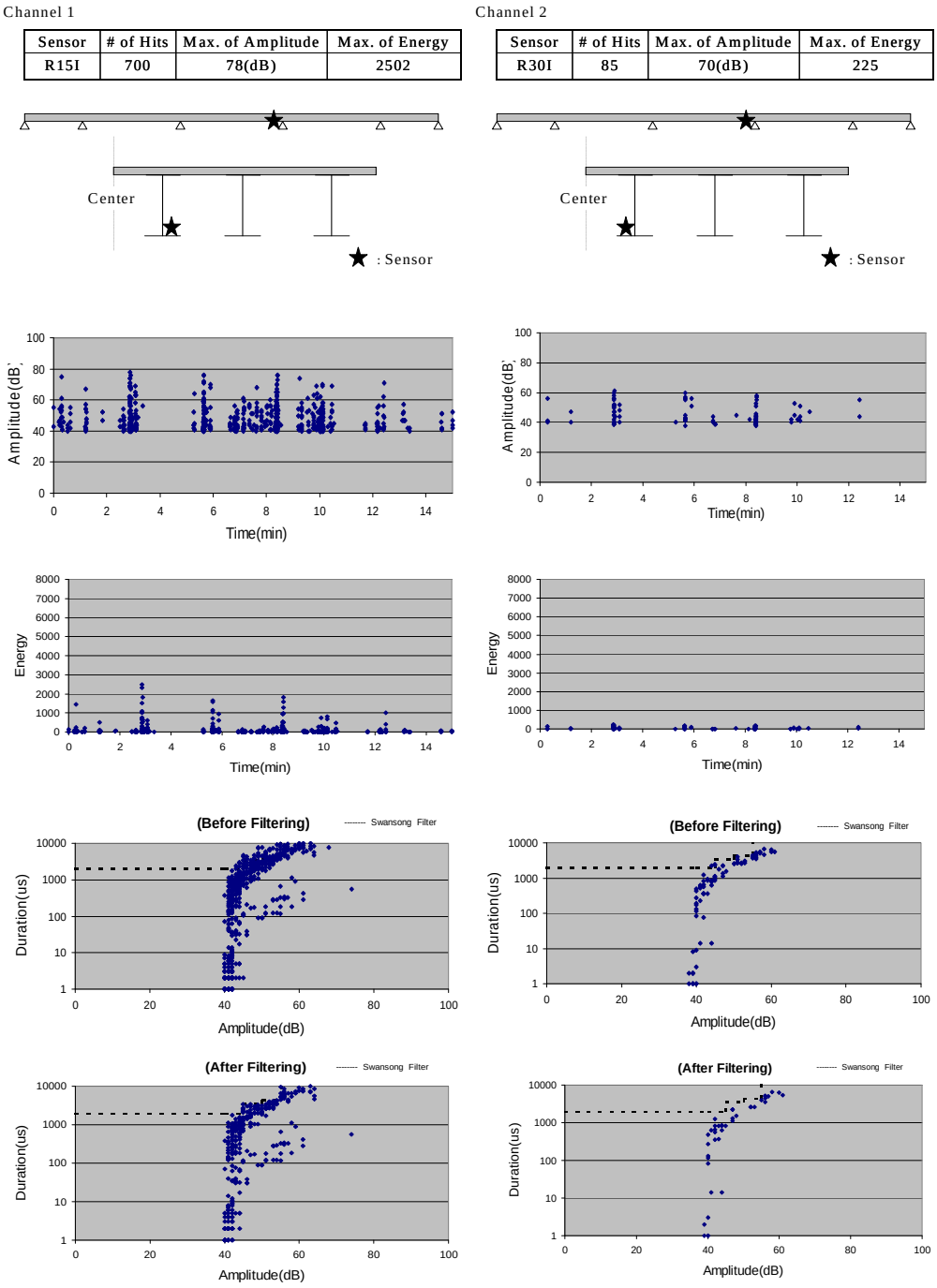

Figure 3.15 Period 6 (Texas-71 Bridge over US-183)

As was the results at the I-35 Bridge, the R30I sensor did not capture as much noise as the R15I sensor and the swansong filter didn't improve the data drastically. The Swansong II and III Filter did eliminate the noise data by 47% and 34% on average respectively. The maximum amplitude of the signal was about 70 dB for R30I, 80 dB for R15I. As the Period 1 through 4 indicates, the mid-span of the girder is less noisy than the support for both of R15I and R30I. This suggests that the noise is likely coming mainly from the support and go through the entire girder.

3.5 Noise Discrimination Procedure

Noise discrimination procedures are considered as follows:

(1) Frequency discrimination

The R30I sensor , the higher frequency transducer, may be the best choice because it was less sensitive to noise than the R15I sensor. On the other hand, the R30I sensor is less sensitive to the signal originating from the crack due to the higher attenuation of the higher frequency signals. This was confirmed in the laboratory test result (see Section 5.4.1).

(2) Threshold

Because genuine data may be ignored, it's not a good idea to raise the threshold too high.

(3) Swansong Filter

Judging from the results of this background noise monitoring, the Swansong Filter is useful to a certain extent. However, there seems to be noise due to impact of moving vehicles which cannot be eliminated by the Swansong Filter.

(4) Spatial filtering (guard sensor)

Since we know the interest area (the location of an intentional crack) of the specimen for our field test, spatial filtering may be the effective way for noise discrimination.

In conclusion, it seems reasonable to adopt spatial filtering as a noise discrimination procedure using R15I sensors. Results using this technique are presented in Chapter 6.

CHAPTER 4. STRESS MEASURING

4.1 Introduction

In order to duplicate field conditions in the laboratory and verify that the crack is long enough to grow in the field, it is necessary to know an actual stress range of the bridge where the continuous AE monitoring was performed. The flange stress was measured on the Tesxas-71 Bridge over US-183 (see Figure 3.3) to determine the stress range for the laboratory test.

4.2 Experimental Program

4.2.1 Instrumentation

The stress measurement was conducted by measuring the strains using electrical-resistance strain gauges, Tokyo Sokki Kenkyujo Cooperation FLA-10-11. The stress was calculated by multiplying the strain with Young's modulus of steel (29×10^6 psi). Strain data were collected using a Campbell Scientific, INC CR9000 Measurement and Control data acquisition system.

Figure 4.1 Instrumentation

4.2.2 Test Program

Two strain gauges were attached on the lower flange at mid-span of the 2nd and 3rd girder respectively. The strain data were recorded for 10-minute intervals at a rate of 100 samples/second. This was repeated 6 times under the normal bridge traffic.

4.3 Test Results for the Stress Measuring

The maximum and minimum stresses of each 10-minute measuring period are tabulated in Table 4.1. Note the actual stress level is all positive due to positive dead load stresses. The data is the change in stress due to the live load. One of the 10-minute measuring results is shown in Figure 4.2. Figure 4.3 indicates fluctuation in the stress during the 10 seconds when the maximum stress occurs. The positive stress values indicate tensile stresses whereas negative values indicate compressive stresses.

Table 4.1 Maximum and Minimum Stresses

	2nd girder			3rd girder		
	Max. (ksi)	Min. (ksi)	S_R (ksi)	Max. (ksi)	Min. (ksi)	S_R (ksi)
Period 1	1.752	-0.841	2.593	2.821	-1.204	4.025
Period 2	3.181	-1.195	4.376	2.596	-1.095	3.691
Period 3	1.971	-0.659	2.630	1.962	-0.629	2.591
Period 4	1.997	0.892	2.889	2.116	-1.656	3.772
Period 5	2.464	-0.743	3.207	2.431	-1.431	3.862
Period 6	2.874	-1.211	4.085	2.897	-1.311	4.208

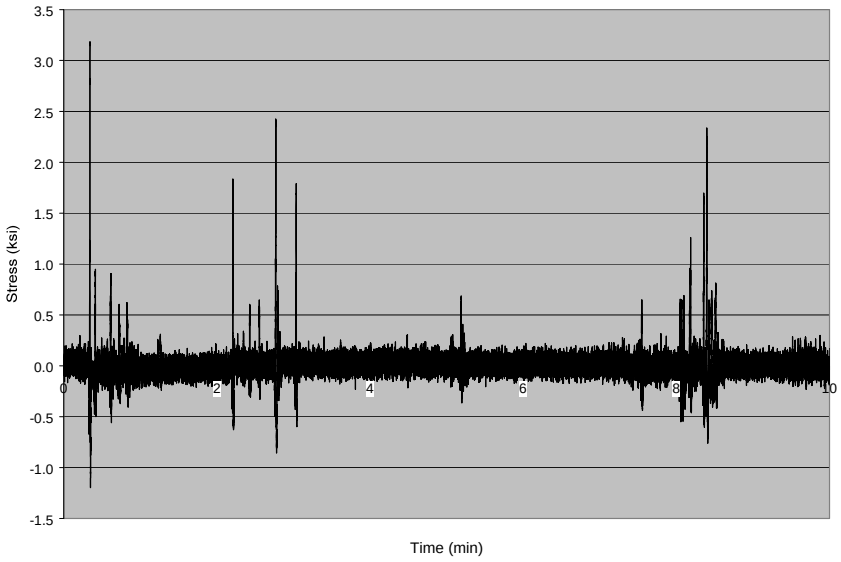

Figure 4.2 Stresses of 10-minute Measuring (Period 2, 2nd girder)

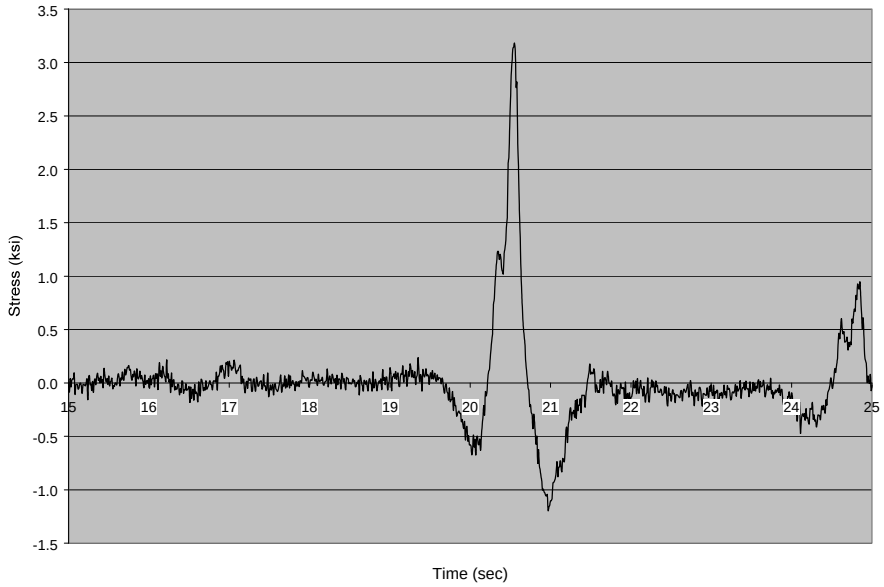

Figure 4.3 Stress Variation During 10 Seconds (Period 2, 2nd girder)

The stress variation shown in Figure 4.3 was the expected form which matches the influence line for the moment at the center span of the continuous beam. This justifies the validity of the results that the stresses were generated by moving vehicle loads. The maximum stress range for the event in Figure 4.3 is 4.4 ksi. Judging from these results, 3 ksi was selected as a reasonable value to use as a stress range for the laboratory test.

CHAPTER 5. LABORATORY TEST

5.1 Introduction

Two types of continuous AE monitoring of fatigue crack growth were performed. The primary objectives of the first test were to confirm the correlation between propagating fatigue cracks and AE parameters as well as to identify the difference attributed to the type of sensors. The primary objectives of the second test were to identify the crack growth and the crack location by AE activity using the guard sensor technique and source location technique and compare those results with the field test. The two specimens were loaded differently. In the first fatigue test the specimen was loaded directly by gripping the cracked plate, while in the second fatigue test the specimen was subjected to cyclic loading by clamping it to a bigger steel plate which was intended to simulate the flange of the bridge.

5.2 Experimental Program for AE Monitoring of Fatigue Crack Growth (1)

5.2.1 Instrumentation

AE were sensed with a 4-channel Physical Acoustic Corporation LOCAN-320 acoustic emission instrument and two sensors (R15I and R30I).

This is the same instrumentation that was used in the background noise study (Chapter 3). The sensor mounting procedure was also the same as used in the background noise study.

5.2.2 Specimen Details

The material used in this experiment as a specimen was 3/32" x 6" plate of low-carbon flat ground stock manufactured by Starrett. The fabrication process for the cracking plate was as follows: first of all, the plate was given an intentional notch (2" deep) by using a hacksaw. Next, this plate was subjected to a stress range of 6 ksi to initiate the fatigue crack and introduce a sharp crack. After cycling at the stress range of 6 ksi, the crack length extended to 3.045". The specimen was then tested at the stress range of 4 ksi. The corresponding stress intensity factor, ΔK, of this specimen (S_R=4 ksi, a/W=3.045/6) is 35.8 ksi-in.$^{1/2}$, which is greater than the estimated threshold, Kth=5.0 ksi-in.$^{1/2}$. This ΔK factor was calculated using the following equation (Okamura 1976):

$$\Delta K = YS_R\sqrt{\pi a}$$

Where
a = Crack Length
W = Specimen Width
S_R = Stress Range

$$Y = \sqrt{\frac{2}{\pi\xi}\tan\frac{\pi\xi}{2}}\,\frac{0.752 + 2.02\xi + 0.37\left(1-\sin\frac{\pi\xi}{2}\right)^3}{\cos\frac{\pi\xi}{2}}$$

$$\xi = \frac{a}{W}$$

The specimen geometry and sensor location is shown in Figure 5.1.

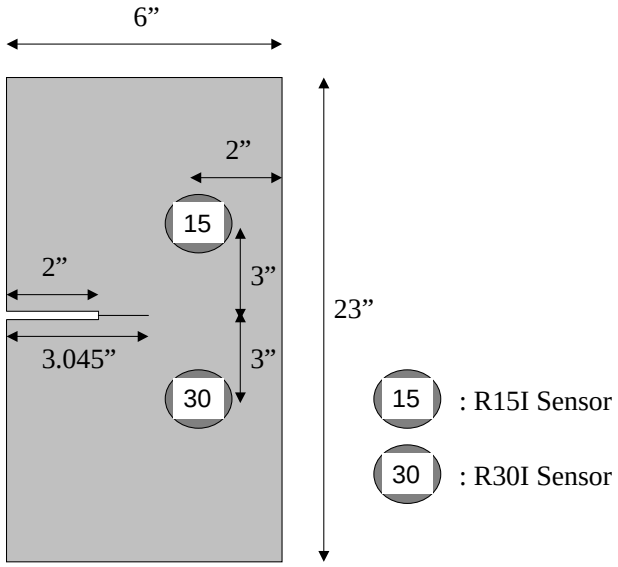

Figure 5.1 Specimen Geometry and Sensor Location (1)

5.2.3 Test Program

This specimen was tested in load control using a model 811 MTS closed-loop fatigue machine. The loading applied to this specimen was positive load ratio only. The stress range (S_R) used in this test was 4 ksi (5 ksi – 1 ksi) and the loading frequency was 3 Hz. The applied force was obtained by multiplying the stress with the gross area of the specimen (3/32”*6”). The cyclic loading and the AE monitoring were interrupted occasionally to measure the crack length. The hardware set up of the AE instrument was the same as in the background noise monitoring (see Table 3.1), except that the threshold was raised to 50 dB. The

dye penetrant method was used to detect the crack tip. This test was continued until the specimen fractured. Figure 5.2 shows an overall view of this test.

Figure 5.2 Overall View of AE Monitoring of Fatigue Crack Growth (1)

5.3 Experimental Program for AE Monitoring of Fatigue Crack Growth (2)

5.3.1 Instrumentation

AE data were collected with an 8-channel Physical Acoustic Corporation Local Area Monitor (LAM) acoustic emission instrument and 4 sensors (R15I). This instrument was developed under a contract from the Federal Highway Administration and has several advantages for field monitoring as compared to conventional ones: it is weather proofed for use outside and can be run by internal batteries. It can be mounted on a bridge as showed in Figure 5.3.

Figure 5.3 Instrumentation (LAM)

5.3.2 Specimen Details

Specimen details were almost the same as in 5.3.1 except for the crack length. Because one of our objectives was to identify the crack growth by AE activity both in the laboratory and in the field and to compare those two results, the crack length needed to be long enough for the crack to grow easily and increase number of AE hits. The crack was generated at a stress range of 6 ksi in the same manner as the first test. After cyclic loading at a stress range of 6 ksi, the crack length was 3.480". The specimen was then tested at the stress range of 3 ksi. The corresponding stress intensity factor, ΔK, (S_R =3 ksi, a/W=3.480/6) is 37.1 ksi-in.$^{1/2}$. The specimen geometry and sensor location is shown in Figure 5.4.

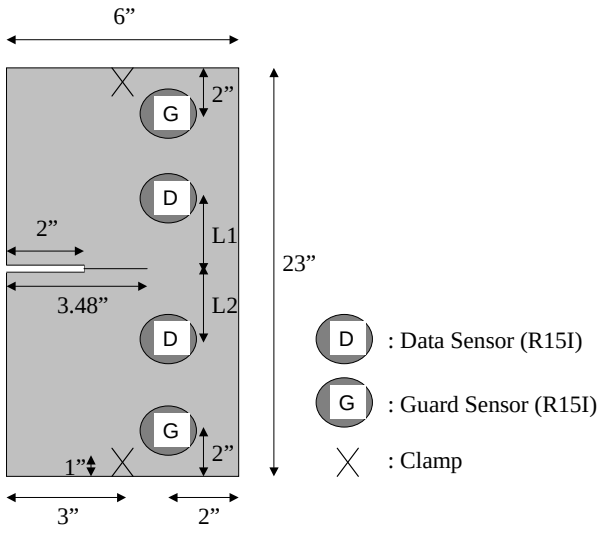

Figure 5.4 Specimen Geometry and Sensor Location (2)

5.3.3 Test Program

The test program was almost the same as in the first test. In this test, however, the specimen was mounted on the bigger steel plate by using two clamps to simulate the field condition. Spacers (3/32" thick plates) were inserted between the specimen and the steel plate to provide clearance. In addition, the guard sensor technique and source location technique were used. The stress range (S_R) used in this test was 3 ksi. Three experiments were performed for 50,000 cycles of loading at a frequency of 1 Hz. The data sensors spacing or the use of guard sensor was varied in each repetition case. In Case 1 the sensors spacing was symmetrical with respect to the crack location and the guard sensor was on. In Case 2 the sensors spacing was symmetrical and the guard sensor was off. In Case 3 the sensors spacing was unsymmetrical and the guard sensor was on. The comparison between Case 1 and Case 2 was done to determine the effect of the guard sensor, and the comparison between Case 1 and Case 3 to determine the effect of the crack location. Data sensors and guard sensors were located linearly as shown in Figure 5.4. The specimen was clamped at 1" from the both ends, while guard sensors were located at 2" from the ends (see Figure 5.5). This means that noise coming from outside the specimen is supposed to be captured by guard sensors before being captured by data sensors. Figure 5.6 shows the specimen in the machine. Crack length was measured at the end of each fatigue test. Gain of transducers was adjusted within $\pm$3 dB with respect to 40 dB to keep

the same sensitivity among sensors by using the results of pencil break test. The values of peak definition time, hit definition time and hit lockout time were set in accordance with MONPAC-PLUS Procedure (Monsanto Chemical Company 1992). This procedure is part of an acoustic emission based system for evaluating the structural integrity of metal vessels. Test conditions and the hardware setup are summarized in Table 5.1 and Table 5.2 respectively.

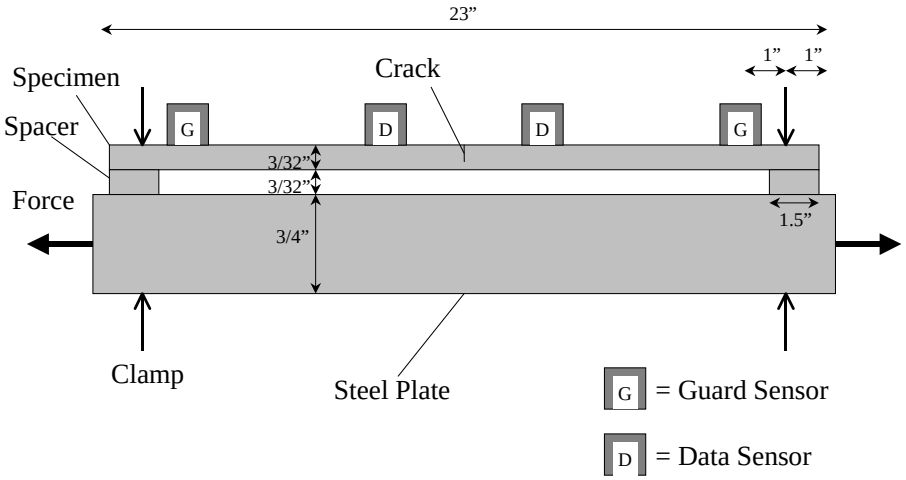

Figure 5.5 Elevation of AE Monitoring of Fatigue Crack Growth (2)

Table 5.1 Test Conditions of the 2nd Laboratory Test

	Case 1	Case 2	Case 3
# of Fatigue Cycles	50,000	50,000	50,000
Loading Frequency	1 Hz	1 Hz	1 Hz
Stress Range	3 ksi (4 ksi – 1 ksi)	3 ksi (4 ksi – 1 ksi)	3 ksi (4 ksi – 1 ksi)
Sensor Spacing	L1 = 3 in. L2 = 3 in.	L1 = 3 in. L2 = 3 in.	L1 = 1.5 in. L2 = 3 in.
Guard Sensor	ON	OFF	ON

Table 5.2 Hardware Set Up

Quantity	Values
Peak Definition Time (PDT)	200 μs
Hit Definition Time (HDT)	400 μs
Hit Lockout Time (HLT)	200 μs
Threshold	50 dB
Gain	40 ±3 dB
Sensor Preamplifier Gain (R15I)	40 dB
Instrument Bandpass Filter	3-400 kHz
Sensor Bandpass Filter (R15I)	100-300 kHz
Wave Velocity	120,000 in./sec
Event Lockout	Case 1,2: 6 in. Case 3: 4.5 in.
Event Over-Calibration	2 in.
Event Timing	First Threshold Crossing (FTC)
Guard Lockout Time	125 μs

Figure 5.6 Overall View of AE Monitoring of Fatigue Crack Growth (2)

5.4 Test Results for Laboratory Test

5.4.1 AE Monitoring of Fatigue Crack Growth (1)

In Figure 5.7 and 5.8, the AE from the fatigue crack in the first specimen, number of hits vs. number of fatigue cycles, cumulative energy vs. number of fatigue cycles, and duration vs. amplitude, of each sensor are shown as well as the crack length. Figure 5.9 shows the fatigue crack.

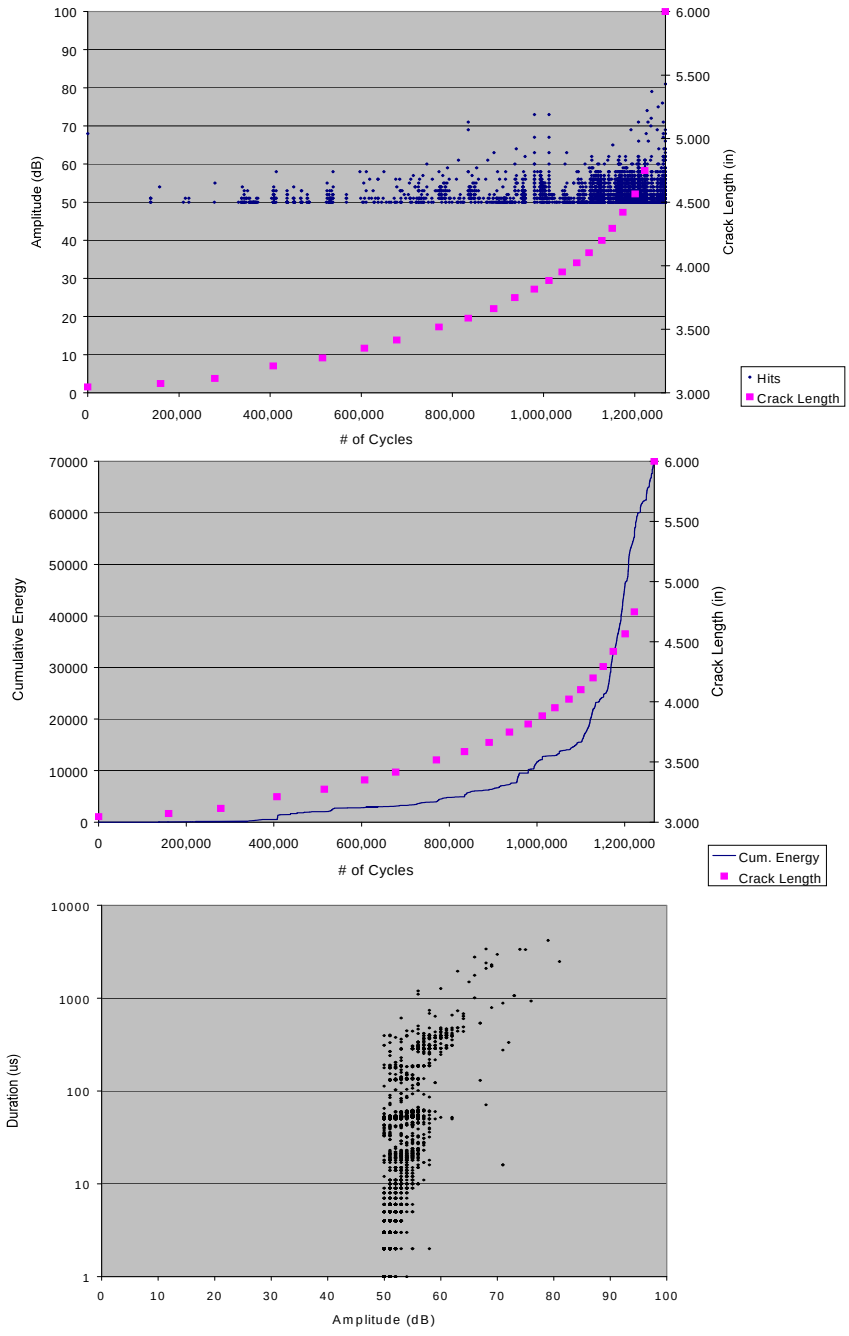

Figure 5.7 AE from Growing Fatigue Crack (R15I)

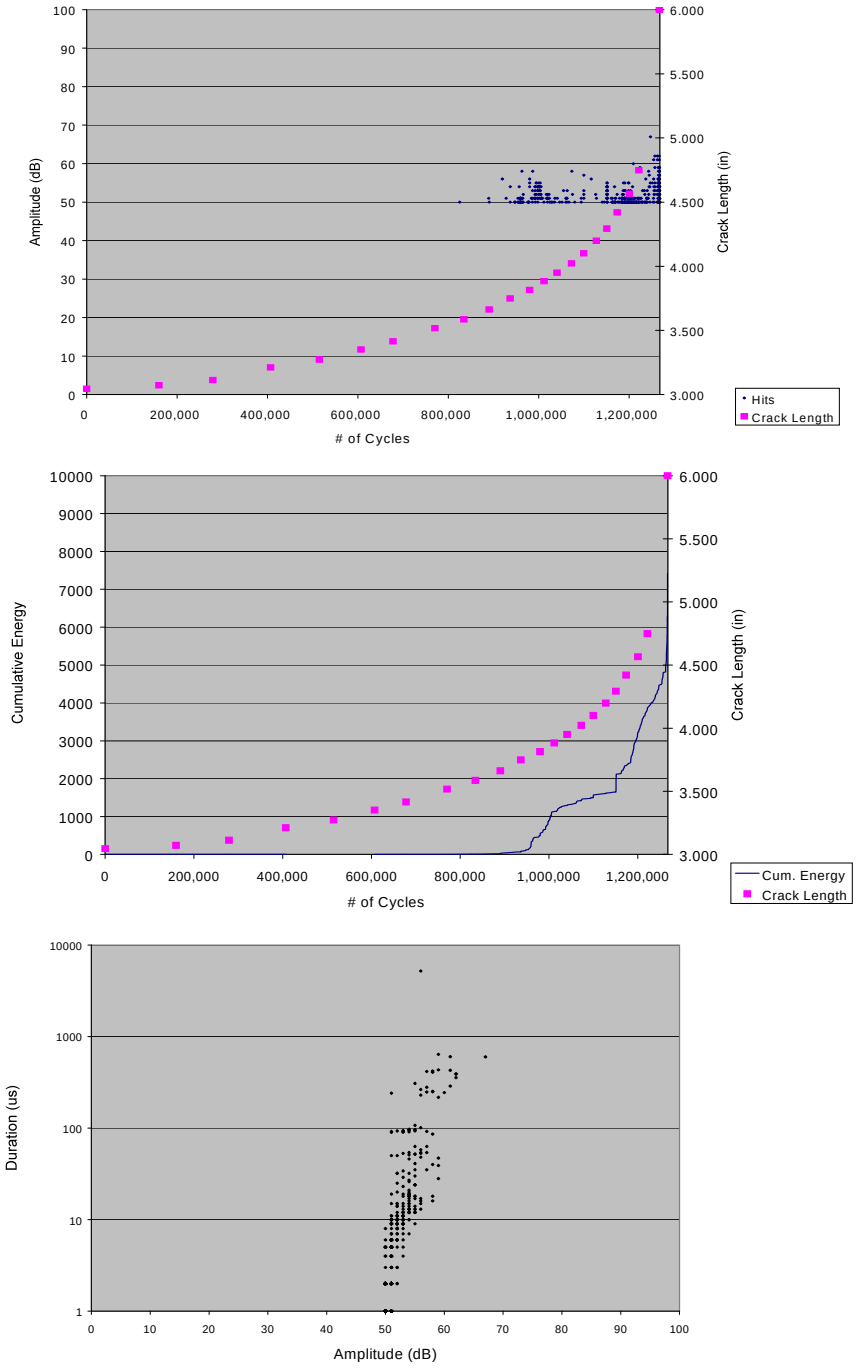

Figure 5.8 AE from Growing Fatigue Crack (R30I)

Figure 5.9 Fatigue Crack

The specimen broke after 1,267,387 fatigue cycles. A large number of hits were obtained by the R15I, while few hits were obtained by the R30I, the higher frequency transducer. The cumulative energy correlated with fatigue crack growth at a high ΔK region.

The cumulative amplitude distribution of the R15I sensor is presented in Figure 5.10 at two stages: after 800,000 cycles and 1,267,387 cycles of loading. Bilinear relation can be seen at the 1,267,387 fatigue cycles, while linear relation can be seen at the 800,000 fatigue cycles. The slopes of these lines are called " b values", which is characteristic of the material and the deformation mechanism (Pollock 1981). Pollock concludes that a steeper slope represents the yielding and a shallow slope represents the crack growth. Therefore according to his interpretation, the deformation mechanism shifted form one mechanism

(yielding) to the combination of two mechanisms (yielding and crack growth) as the number of fatigue cycles increased.

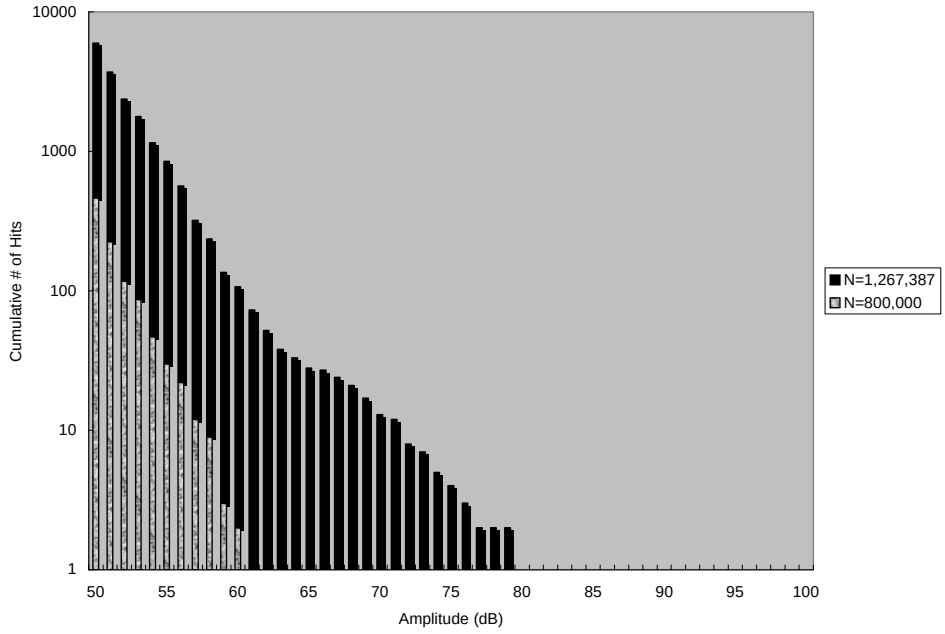

Figure 5.10 Cumulative Amplitude Distribution (R15I)

Figure 5.11 indicates the correlation regarding crack growth rate (da/dN), stress intensity factor (ΔK) and AE hit rate (N') of the R15I sensor.

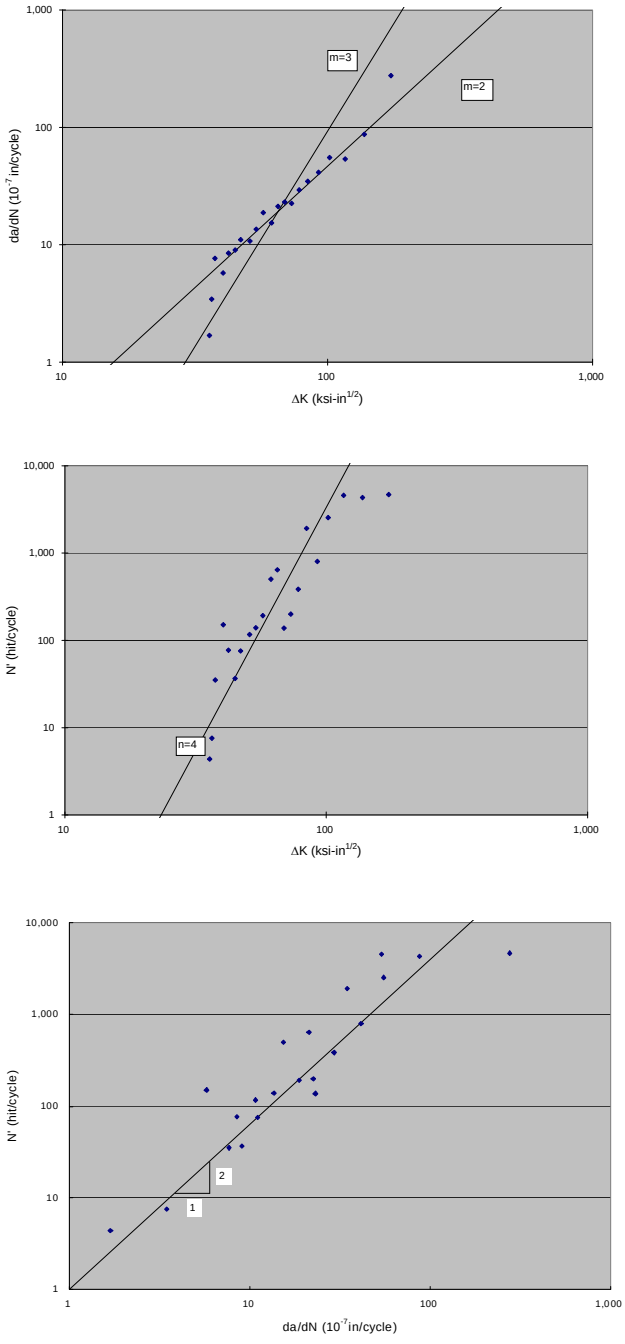

Figure 5.11 Correlation Between Crack Growth and AE (R15I)

It is obvious that correlation between da/dN and ΔK follows the Paris law for crack propagation in fatigue:

$$\frac{da}{dN} = C(\Delta K)^m$$

where C and m are material constants. It has been reported that the correlation between N' and ΔK has similar relationship to the Paris law:

$$N' = A(\Delta K)^n$$

where A and n are also material constants (ASNT 1987 and Morton *et al.* 1973). From Figure 5.11, it appears that the result of this test agree well with the above two relationships. The slopes on the log-log scales were estimated as m=2, n=4 respectively, while typical m value for metals is 3. AE hit rate and crack growth rate were correlated, but with a larger scatter in the results. The approximate slope was 2.

5.4.1 AE Monitoring of Fatigue Crack Growth (2)

Figure 5.12 through Figure 5.14 show the location displays; and Figure 5.15 through Figure 5.17 show the graphs of duration vs. amplitude observed in each case.

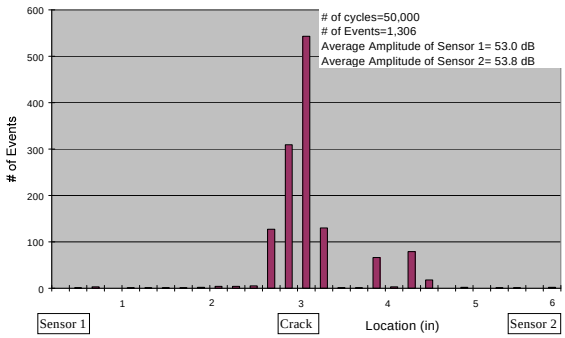

Figure 5.12 Location Display (Case 1)
[Symmetrical Sensor Spacing, Guard Sensor On]

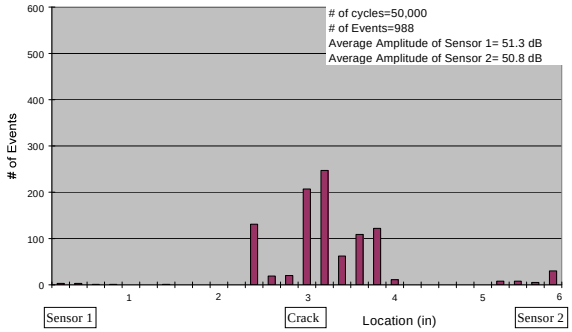

Figure 5.13 Location Display (Case 2)
[Symmetrical Sensor Spacing, Guard Sensor Off]

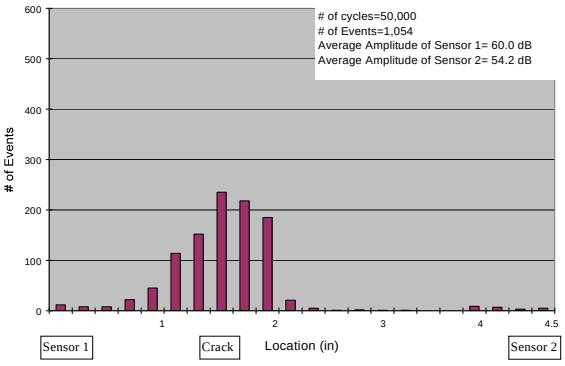

Figure 5.14 Location Display (Case 3)
[Unsymmetrical Sensor Spacing, Guard On]

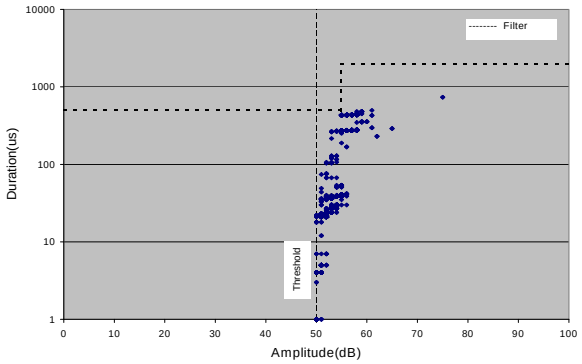

Figure 5.15 Duration-Amplitude (Case 1)
[Symmetrical Sensor Spacing, Guard On]

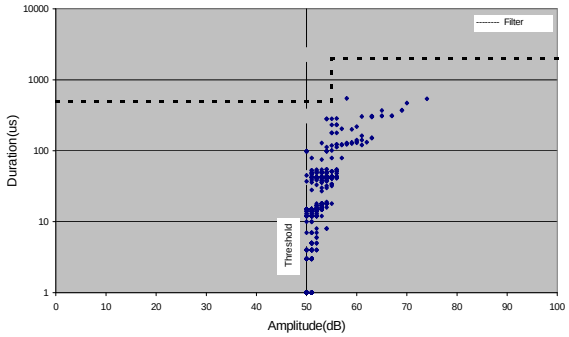

Figure 5.16 Duration-Amplitude (Case 2)
[Symmetrical Sensor Spacing, Guard Sensor Off]

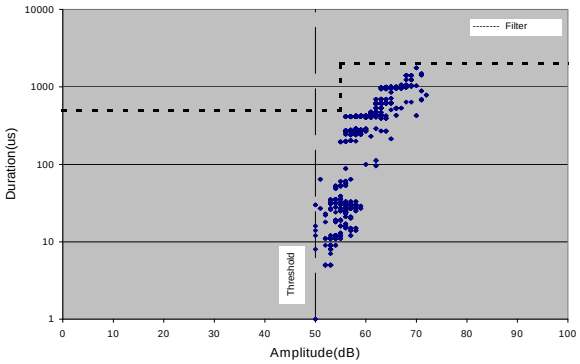

Figure 5.17 Duration-Amplitude (Case 3)
[Unsymmetrical Sensor Spacing, Guard Sensor On]

The linear location technique provided good location displays even when no guard sensors were used and when the data sensors spacing was unsymmetrical as indicated in Figure 5.12 through Figure 5.14. The number of events was almost the same in each case; about 1000. Location display of Case3 was less precise compared with Case 1 or Case2. One possible reason for lower precision in Period 3 monitoring may be the closeness of sensor 1 to the crack. In this case, the size of the sensor is significant compared to the distance of travel of the wave. AE hits tended to be less than 1000μs in duration and less than 70 dB in amplitude in each case as indicated in Figure 5.15 through Figure 5.16. Judging from the similarity in data quality (duration vs. amplitude) as well as in location display of Case 2 to other two cases, there was little influence of noise in the laboratory.

Apparent crack growth was not found during any of three cases. It is possible that some of the AE recorded in these tests were generated from the rubbing of the fracture surfaces. Another possibility is that slight yielding at the crack tip generated some emissions. Although one of the initial objectives was to identify the crack growth by using AE parameters, it cannot be discussed here because of lack of information. Nonetheless, it can be stated that good source location is obtained without significant crack growth.

It is noted that the good source location heavily relied on the loading frequency. In preliminary tests with the loading frequency set at 3 Hz or more,

AE events from the crack were buried in AE events due to the background noise even though the guard sensors were on.

A filter is defined in the plots of duration vs. amplitude. This will be discussed in the next chapter.

CHAPTER 6. FIELD TEST

6.1 Introduction

Field AE monitoring was conducted at the Texas-71 Bridge over US-183 (see Figure 3.2). Two types of specimen were used for this test; one was a cracked plate, identical with the one of laboratory test, the other was a plane plate. These specimens were mounted on the bridge by using clamps and monitored continuously under the normal bridge traffic conditions using the guard sensor technique and source location technique.

6.2 Experimental Program

Basically, the same experimental program as in the second laboratory test (see section 5.2) was repeated in this field test. The cracked plate from the second laboratory test was mounted on this bridge (see Figure 5.4). In addition to the cracked plate, an uncracked plate with the same plane geometry (6"*23") was monitored using the same sensor location as the cracked plate. Two specimens were mounted on the both sides of the lower flange at the mid-span of the 3rd girder by clamps and the LAM (AE data acquisition system) was set at the support as shown in Figure 6.1. Spacers (3/32" thick plates) were inserted between the specimens and the flange of the girder to provide clearance. AE data

were recorded using 8 sensors (R15I) under the normal traffic condition for a total of 30 hours. The monitoring intervals of the 3 periods were 12 hours, 6 hours, and 12 hours respectively. Data sensors spacing and guard sensor usage was altered in the three intervals. The LAM was run by internal batteries, which were charged by a generator occasionally during the test. The only difference of the hardware setup between this field test and the second laboratory test was threshold. Since only a few events were recorded in preliminary monitoring with the threshold set at 50 dB, it was lowered to 45 dB in order to raise system sensitivity. Crack length was measured at the end of every interval. Test conditions are summarized in Table 6.1. L1, L2 and the guard sensor position are as defined in Figure 5.4.

Table 6.1 Test Conditions of the Field Test

	Period 1	Period 2	Period 3
Monitoring Intervals	12 hours	6 hours	12 hours
Specimen	Cracked Plate Plane Plate	Cracked Plate Plane Plate	Cracked Plate
Sensor Spacing	L1 = 3 in. L2 = 3 in.	L1 = 3 in. L2 = 3 in.	L1 = 1.5 in. L2 = 3 in.
Guard Sensor	ON	OFF	ON

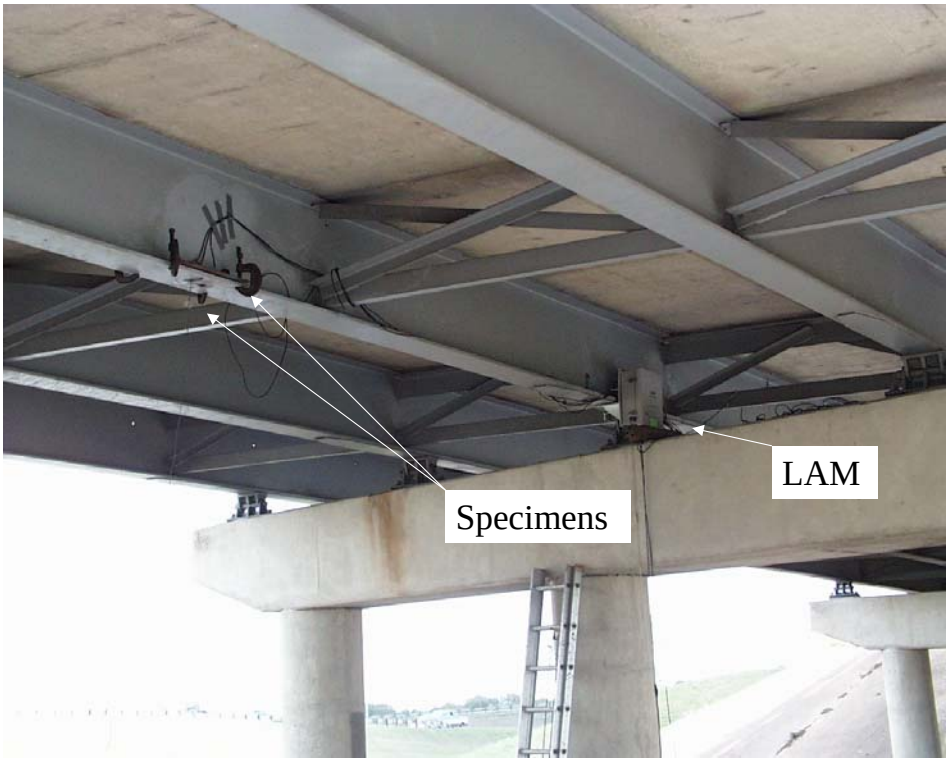

Figure 6.1 Overall View of Field Test

6.3 Test Results for the Field Test

Figure 6.2 through Figure 6.6 show the location displays, and Figure 6.7 through Figure 6.11 plot duration vs. amplitude of each period.

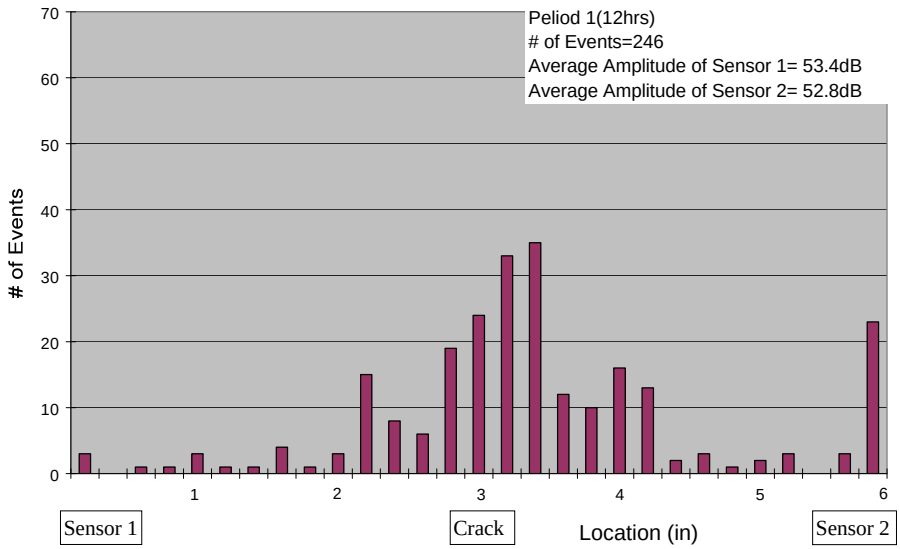

Figure 6.2 Location Display (Period 1, Cracked Plate)
[Symmetrical Sensor Spacing, Guard Sensor On]

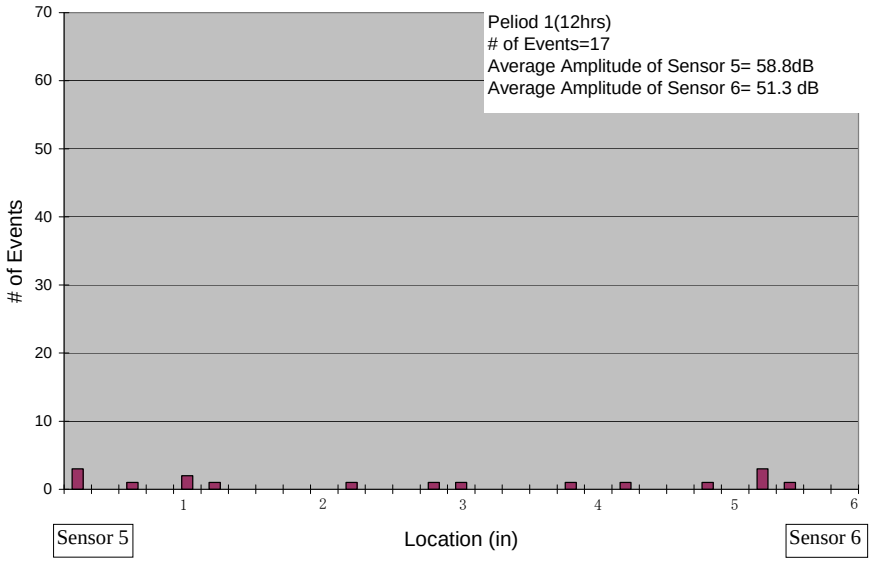

Figure 6.3 Location Display (Period 1, Plane Plate)
[Symmetrical Sensor Spacing, Guard Sensor On]

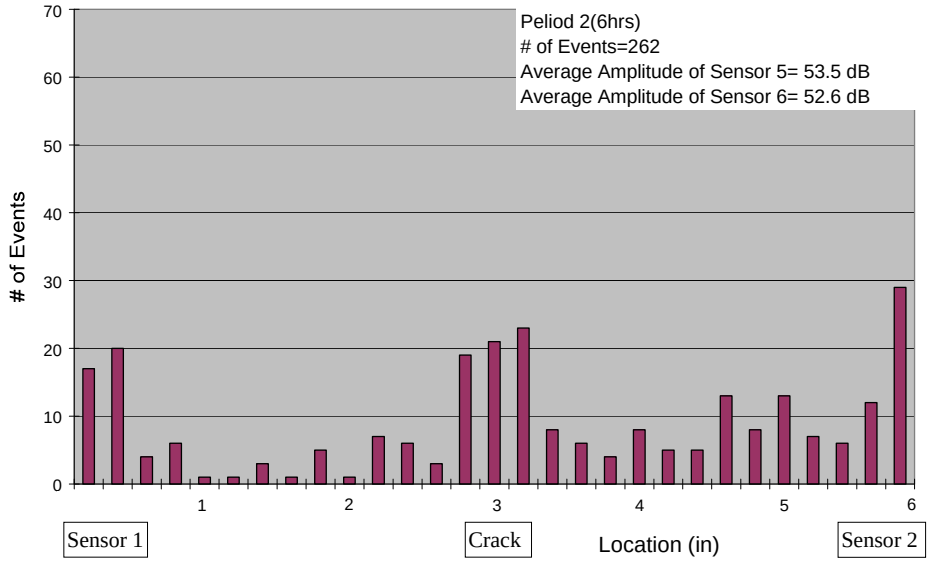

Figure 6.4 Location Display (Period 2, Cracked Plate)
[Symmetrical Sensor Spacing, Guard Sensor Off]

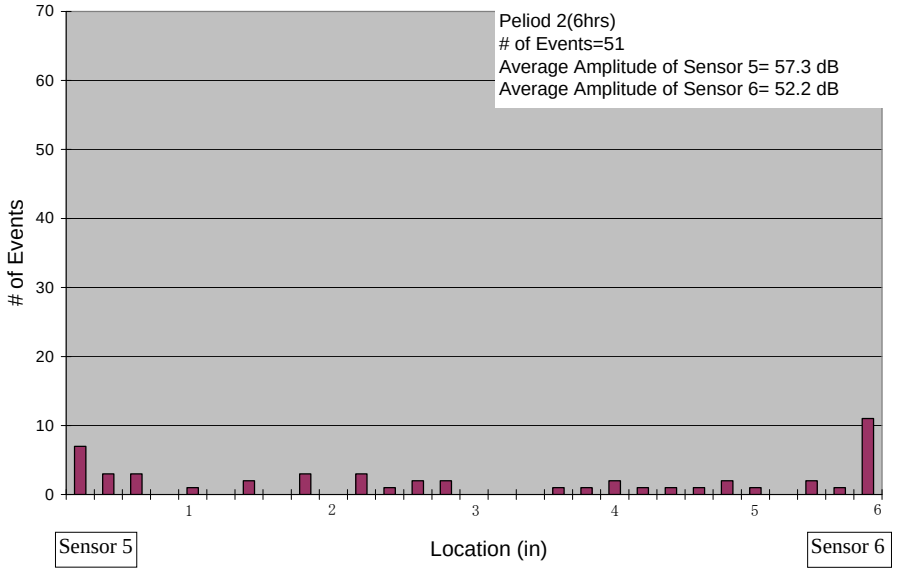

Figure 6.5 Location Display (Period 2, Plane Plate)
[Symmetrical Sensor Spacing, Guard Sensor Off]

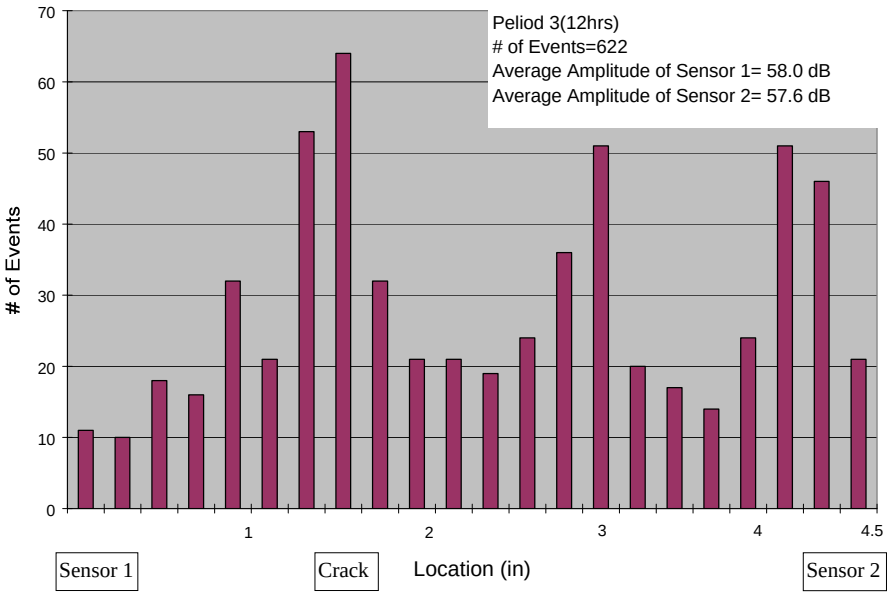

Figure 6.6 Location Display (Period 3, Cracked Plate)
[Unsymmetrical Sensor Spacing, Guard On]

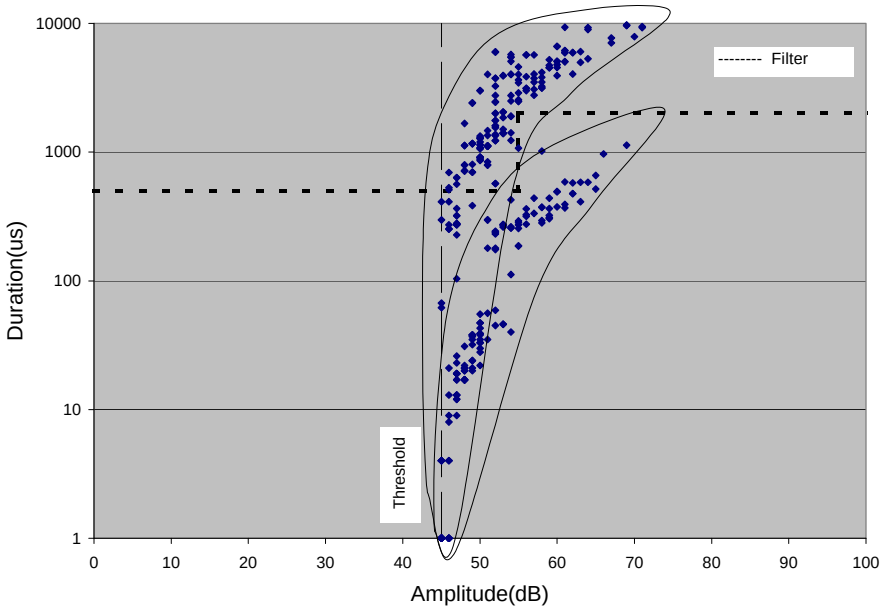

Figure 6.7 Duration-Amplitude (Period 1, Cracked Plate)
[Symmetrical Sensor Spacing, Guard On]

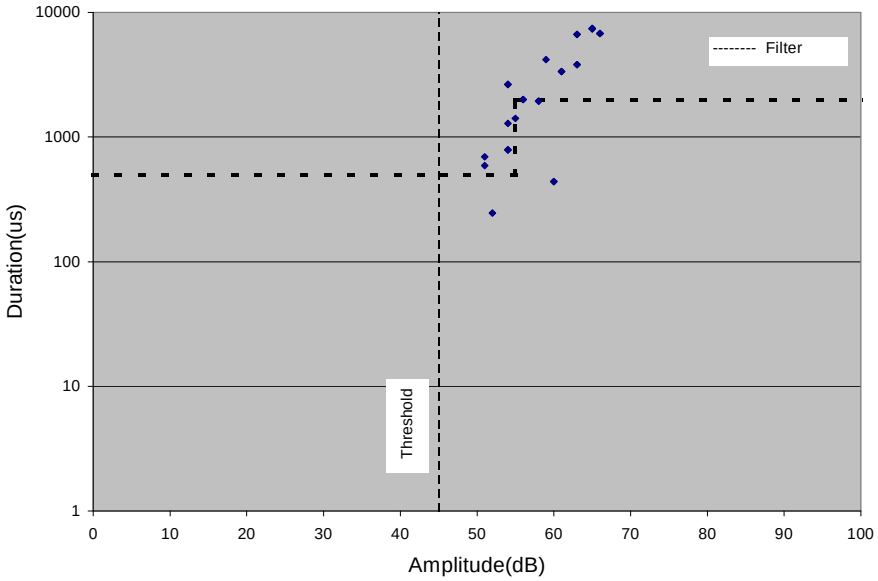

Figure 6.8 Duration-Amplitude (Period 1, Plane Plate)
[Symmetrical Sensor Spacing, Guard On]

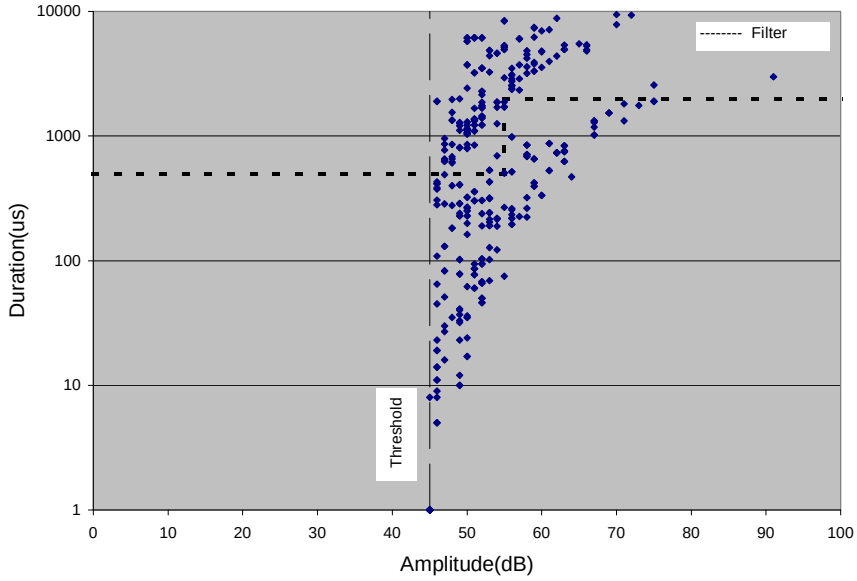

Figure 6.9 Duration-Amplitude (Period 2, Cracked Plate)
[Symmetrical Sensor Spacing, Guard Off]

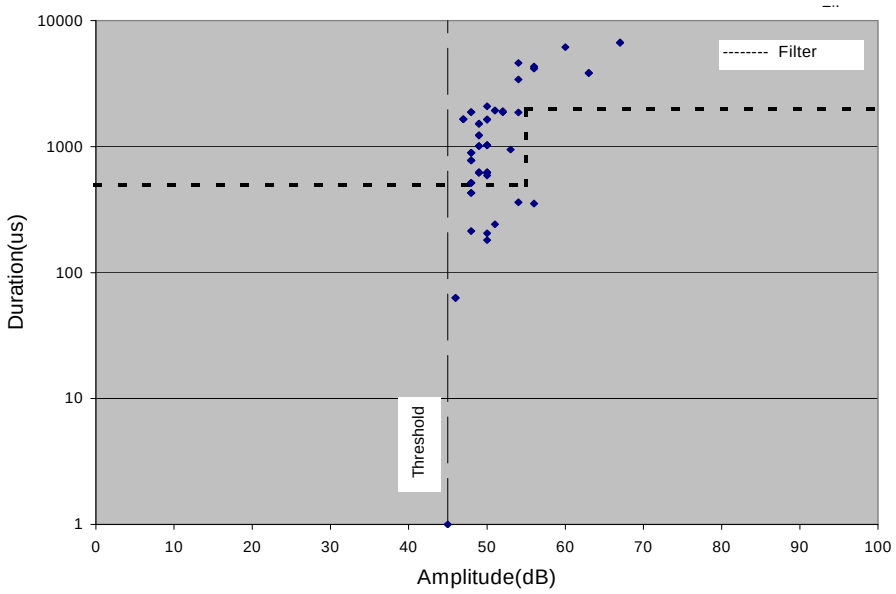

Figure 6.10 Duration-Amplitude (Period 2, Plane Plate)
[Symmetrical Sensor Spacing, Guard Off]

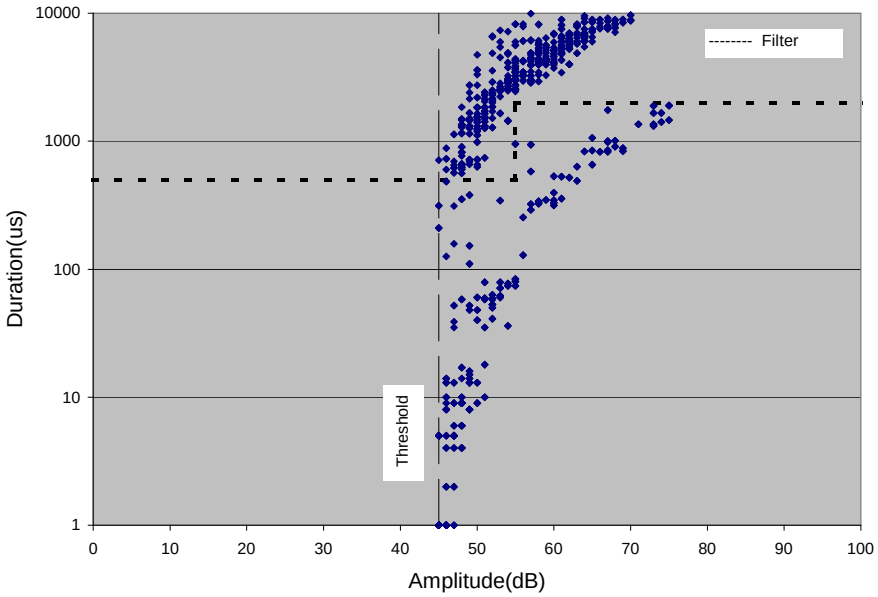

Figure 6.11 Duration-Amplitude (Period 3, Cracked Plate)
[Unsymmetrical Sensor Spacing, Guard Sensor On]

The location displays of the cracked plate show the crack position as a peak of events, even though they are not as sharp as observed in the laboratory test. Judging from the sufficiency of 6-hours monitoring in Period 2, 6 hours is long enough to determine the existence and location of the crack in this specimen. Comparison between Period 1 and Period 2 indicates that the guard sensors worked well. Several events at locations of other than the crack position were extracted in the cracked plate, especially in Period 3, while only a few of misleading events were found in the plane plate in Period 1 and Period 2 as well as in the second laboratory test. The reason for the difference in the misleading events between the cracked plate and the plane plate is not clear. One possible reason for those misleading events may be the reflections of the wave, which originated from the crack, from the edge of the specimen. The multiple hits from the reflections may generate misleading events in a small specimen (Wagner, Huber, Fowler and Crump 1992). However, the reason for the difference in the misleading events between the cracked plate in this field test and the second laboratory is not well understood. There might be the effect of extraneous noise due to traffic.

In the plots of duration vs. amplitude of the cracked plate two diagonal bands running from lower left to upper right can be recognized as indicated in Figure 6.7. Since the lower band corresponds to the results of the second laboratory test (see Section 5.4.1) and the upper band corresponds to the one of

the background noise monitoring (see Chapter 3), it seems possible to assume that the upper band was mainly caused by extraneous noise and the lower band by the crack. This hypothesis can be also supported by the concept of the Swansong Filter described in 2.3.1, which states that false hits due to extraneous noise have long duration and low amplitude. One of the results of the background noise monitoring is showed in Figure 6.12. The majority of the hits have longer duration and low amplitude.

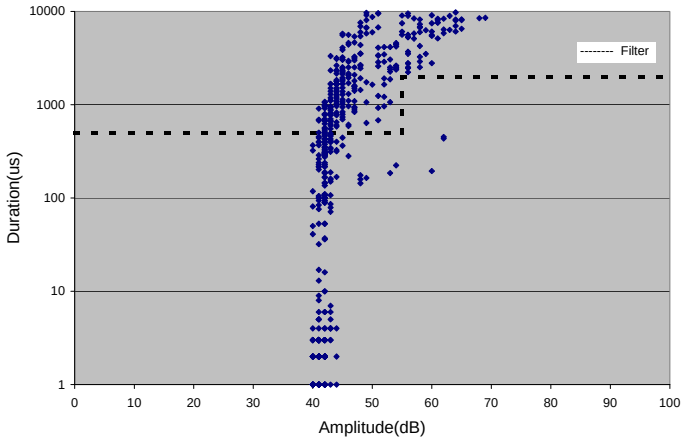

Figure 6.12 Result of the Background Noise Monitoring
[Period 5, Texas-71 Bridge, Ch.1]

In order to eliminate the events due to hits of the upper band, a filter showed in the plots of duration vs. amplitude by broken lines was tried. The filter is defined as follows:

If A_i<55 dB and D_i>0.5 ms
or D_i>2 ms
eliminate all hits

where for given hit I:
A_i = Amplitude (dB)
D_i = Hit Duration (ms)

The filter eliminated the noise data of Figure 6.12 by 57%, while the Swansong II Filter can by 54% and Swansong III Filter by 31%.

Figure 6.12 through Figure 6.16 show the location displays after applying the above filter.

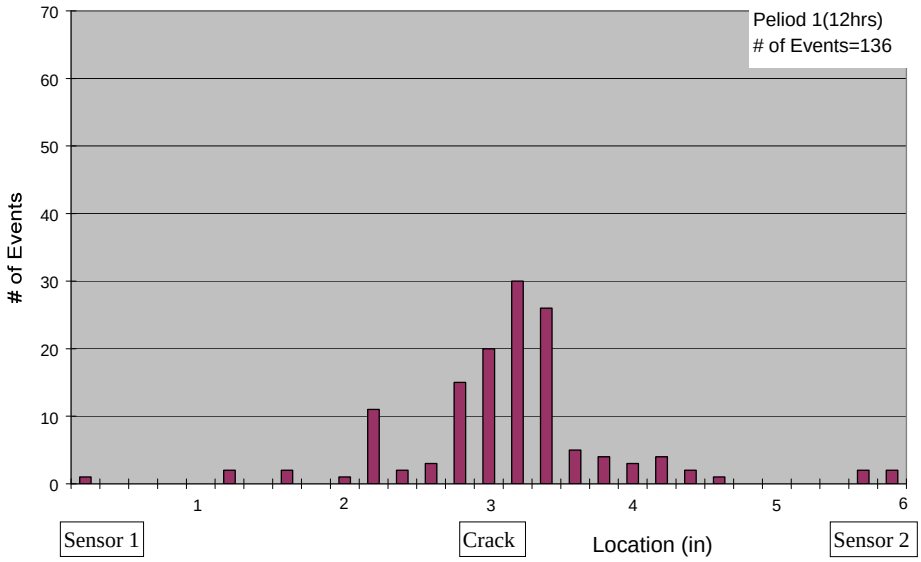

Figure 6.12 Location Display (Period 1, Cracked Plate, After Filtering) [Symmetrical Sensor Spacing, Guard Sensor On]

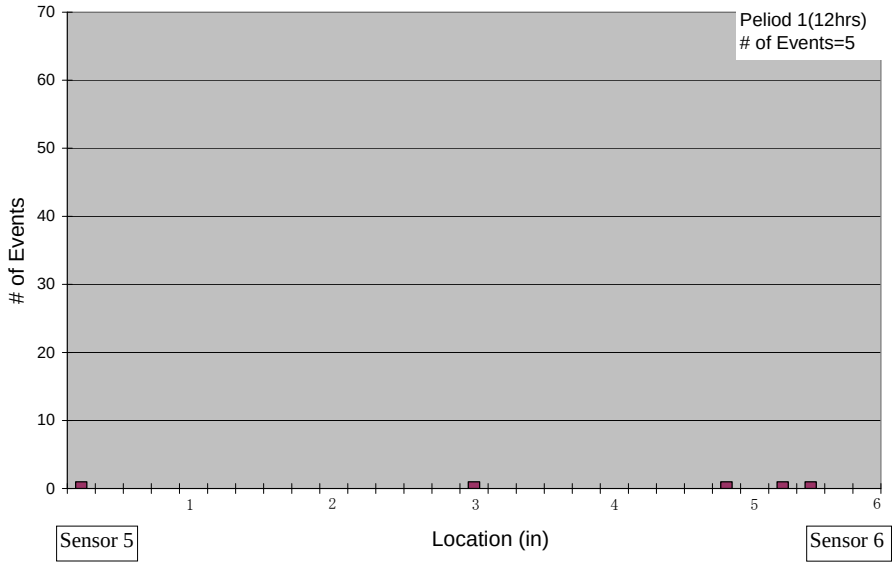

Figure 6.13 Location Display (Period 1, Plane Plate, After Filtering) [Symmetrical Sensor Spacing, Guard Sensor On]

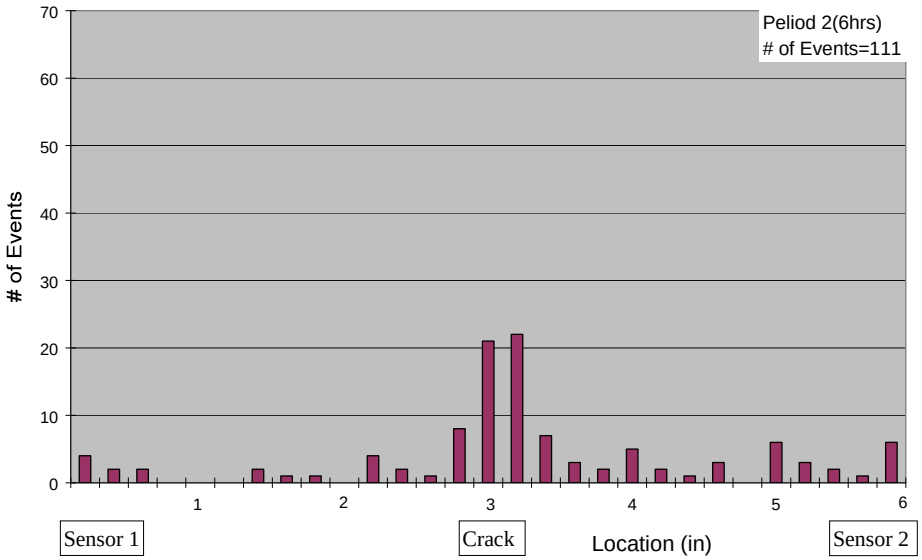

Figure 6.14 Location Display (Period 2, Cracked Plate, After Filtering)
[Symmetrical Sensor Spacing, Guard Sensor Off]

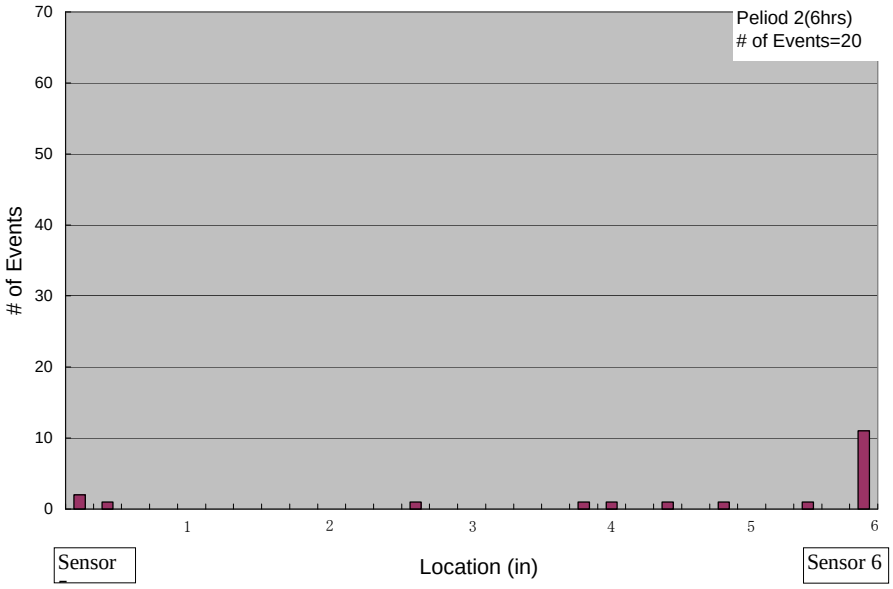

Figure 6.15 Location Display (Period 2, Plane Plate, After Filtering)
[Symmetrical Sensor Spacing, Guard Sensor Off]

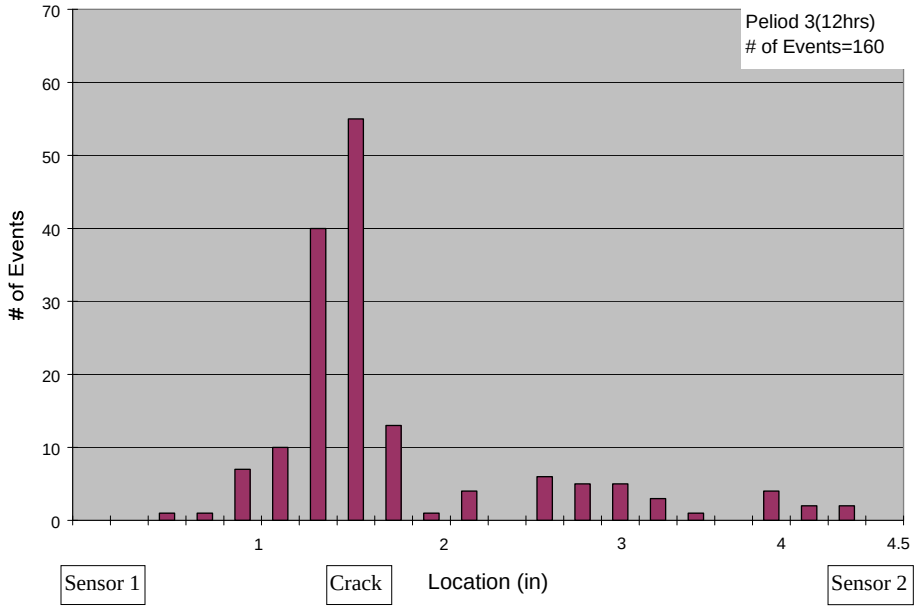

Figure 6.16 Location Display (Period 3, Cracked Plate, After Filtering)
[Unsymmetrical Sensor Spacing, Guard On]

The filter successfully distinguishes the events due to the crack from the ones due to other sources, especially in Period 3 even though some misleading events still remain. Accordingly it may be stated that the upper band in the plots of duration vs. amplitude was mainly caused by extraneous noise and the lower band by the crack. However, the effect of reflections from the edge of the specimen must also be considered: AE hits in the upper band may contain multiple hits from reflections of the wave originated from the crack.

No apparent crack growth was found. The correlation between fatigue crack growth and AE parameters is not clear, either. However, good source

location was obtained without significant crack growth in the field as well as in the laboratory.

CHAPTER 7. CONCLUSIONS AND RECOMMENDATIONS

7.1 Conclusions

This research explored the correlation between fatigue crack growth and AE parameters as well as the ability to detect the fatigue cracks by using AE activity both in an in-service bridge and in the laboratory. After performing the background noise monitoring of bridges in the field and continuous AE monitoring of fatigue crack in the laboratory and in the bridge, the following major conclusions were obtained:

(1) Although the Swansong II Filter did eliminate the noise data by about 50 %, it could not eliminate the traffic noise data completely. The remaining data seem to come mainly from the impact of the moving vehicles.

(2) The R15I sensor, the lower frequency transducer, was more sensitive to the fatigue crack growth than the R30I sensor, the higher frequency transducer, in the first laboratory test.

(3) The cumulative energy correlated with fatigue crack growth at a high ΔK region in the first laboratory test.

(4) The correlations, which have been reported by others, between crack growth rate, stress intensity factor and AE hit rate were reaffirmed in the first laboratory test.

(5) There was little influence of noise in the laboratory.

(6) It was successfully demonstrated that the source location technique located the crack position clearly without significant crack growth both in the field and in the laboratory.

(7) The guard sensors screened out noise signals from outside the specimen in the field.

(8) 6-hours monitoring was long enough to identify the existence and location of the crack in the field.

(9) A specific filter based on the relationship between duration and amplitude successfully eliminated most of the extraneous noise and drastically improved the location display in the field test.

7.2 Recommendations

The results of this research indicate that AE method is able to clearly and reliably detect the existence and the location of the deep crack (ΔK= 37.1 ksi-in.$^{1/2}$) in the plate. This suggests that the AE method could be a good inspection tool for in-service steel bridges.

The recommendations for AE method to be a useful steel bridge inspection tool are as follows:

(1) Use of stress data

It may be useful to know when AE is generated. By using stress data, it is able to distinguish the AE related to the crack growth from AE due to other AE emitting phenomenon.

(2) Data accumulation

The detection of cracks with low values of stress intensity factor (ΔK) as well as the detection of crack initiation and growth are unsettled questions. In addition, the detection of the crack in a complicated joint area, where the fatigue crack is most likely to occur, is still a doubtful. A variety of AE data patterns to characterize the flaw condition may result in a standard inspection procedure.

(3) Incorporation of AE method into BMS (Bridge Management System)

In the broad sense BMS is considered as an integrated system to optimize the strategies for inspection and maintenance program using a variety of databases. AE data can be one of the fundamental parameters. In order to incorporate AE to BMS, methods to automatically process a large amount of data without subjective inspector interpretation must be developed.

References

Adams, N. J. I. (1972). "Fatigue Crack Closure at Positive Stresses." *Engineering Fracture Mechanics*, 4(3), 543-554.

Bray, D. E., & Stanley, R. K. (1997). Nondestructive Evaluation - A Tool in Design, Manufacturing and Service, CRC Press.

Chase, S. B. (1995). "NDE for Steel Bridges." *Civil Engineering*, American Society of Civil Engineering, 65(5), 233-234.

Frank, K. H. (1993). "Nondestructive Evaluation Problems in Steel Bridges." Conference on Nondestructive Evaluation of Bridges, August 25-27, 1992. Federal Highway Administration.

Lozev, M. G., & Clemeña, G. G., & Duke, J. C. Jr., & Sison, M. F. Jr., & Horne, M. R. (1997). Acoustic Emission Monitoring of Steel Bridge Members, Final Report, Virginia Transportation Research Council.

MONPAC-PLUS Procedure for Acoustic Emission Testing of Metal Tanks/Vessels, Draft D, August 1992, Monsanto Chemical Company (1992).

Morton, T. M., & Harrington, R. M., & Bjeletich, J. G. (1973). "Acoustic Emission of Fatigue Crack Growth." *Engineering Fracture Mechanics*, 5(3), 691-697.

Nondestructive Testing Handbook, Second Edition, Vol. 5, Acoustic Emission, ASNT (1987). American Society for Nondestructive Testing.

Okamura, Hiroyuki. (1976). Introduction of Linear Fracture Mechanics (Senkei Hakairikigaku Nyuumon). Tokyo: Baihuukan.

Physical Acoustic Cooperation (PAC). (2000). LAM user's manual Rev 1, PAC Part #: 6310-1000, Associated with: LAM-LOC software for Windows, PAC Part #: 6310-7001 Rev 1 or Higher.

Pollock, A. A. (1995). Acoustic Emission for Bridge Inspection, Application Guidelines, Technical Report, No. TR103-12-6/95, Prepared by Physical Acoustic Corporation for Federal Highway Administration.

Pollock, A. A. (1981). "Acoustic Emission Amplitude Distributions." *International Advances in Nondestructive Testing*, 7, 215-239.

Pollock, A. A., & Smith, B. (1972). "Stress-Wave Emission Monitoring of a Military Bridge." Nondestructive Testing, 30(12), 348-353.

Prine, D. W. (1995). "Problems associated with nondestructive evaluation of bridges". SPIE, 2456, 46-52.

Procedure for acoustic emission evaluation of tank cars and IM-101 tanks. Issue 8. Operation and Maintenance Department, AAR (1999). Association of American Railroads.

Sison, M., & Duke, J. C. Jr., & Clemeña, G., & Lozev, M.G. (1996). “Acoustic Emission: A Tool for the Bridge Engineer.” *Material Evaluation,* American Society of Nondestructive Testing, 54(8), 888-900.

Standard Terminology for Nondestructive Examinations. ASTM E1316-99a. (1999). American Society for Testing and Materials, Philadelphia, Pa.

Wagner, J., & Huber, J., & Fowler, T., & Crump, T. (1992). “Interpretation of Optically Detected Acoustic Emission Signals.” Fourth International Symposium on Acoustic Emission from Composite Materials, July 27-31, 1992. American Society for Nondestructive Testing.